Neurobiology of Disease

Selective Breeding for High Anxiety Introduces a Synonymous SNP That Increases Neuropeptide S Receptor Activity

David A. Slattery,[1]* Roshan R. Naik,[1,3]* Thomas Grund,[1] Yi-Chun Yen,[3] Simone B. Sartori,[4] Andrea Füchsl,[1] Beate C. Finger,[1] Betina Elfving,[5] Uwe Nordemann,[2] Remo Guerrini,[6] Girolamo Calo,[7] Gregers Wegener,[5,9] Aleksander A. Mathé,[8] Nicolas Singewald,[4] Ludwig Czibere,[3] Rainer Landgraf,[3] and Inga D. Neumann[1]

[1]Department of Behavioral and Molecular Neurobiology, and [2]Faculty of Chemistry and Pharmacy, University of Regensburg, 93040 Regensburg, Germany, [3]Max Planck Institute of Psychiatry, 80804 Munich, Germany, [4]Department of Pharmacology and Toxicology, University of Innsbruck, 6020 Innsbruck, Austria, [5]Translational Neuropsychiatry Unit, Department of Clinical Medicine, Aarhus University, DK-8000 Aarhus, Denmark, [6]Department of Chemistry and Pharmaceutical Sciences and Laboratorio per le Tecnologie delle Terapie Avanzate, University of Ferrara, 44100 Ferrara, Italy, [7]Department of Medical Sciences, Section of Pharmacology, National Institute of Neuroscience, University of Ferrara, 44121 Ferrara, Italy, [8]Clinical Neuroscience, Karolinska Institutet, SE-171 77 Stockholm, Sweden, and [9]Pharmaceutical Centre of Excellence, School of Pharmacy, North West University, Potchefstroom, 2520, South Africa

Neuropeptide S (NPS) has generated substantial interest due to its anxiolytic and fear-attenuating effects in rodents, while a corresponding receptor polymorphism associated with increased NPS receptor (NPSR1) surface expression and efficacy has been implicated in an increased risk of panic disorder in humans. To gain insight into this paradox, we examined the NPS system in rats and mice bred for high anxiety-related behavior (HAB) versus low anxiety-related behavior, and, thereafter, determined the effect of central NPS administration on anxiety- and fear-related behavior. The HAB phenotype was accompanied by lower basal NPS receptor (*Npsr1*) expression, which we could confirm via *in vitro* dual luciferase promoter assays. Assessment of shorter *Npsr1* promoter constructs containing a sequence mutation that introduces a glucocorticoid receptor transcription factor binding site, confirmed via oligonucleotide pull-down assays, revealed increased HAB promoter activity—an effect that was prevented by dexamethasone. Analogous to the human NPSR1 risk isoform, functional analysis of a synonymous single nucleotide polymorphism in the coding region of HAB rodents revealed that it caused a higher cAMP response to NPS stimulation. Assessment of the behavioral consequence of these differences revealed that intracerebroventricular NPS reversed the hyperanxiety of HAB rodents as well as the impaired cued-fear extinction in HAB rats and the enhanced fear expression in HAB mice, respectively. These results suggest that alterations in the NPS system, conserved across rodents and humans, contribute to innate anxiety and fear, and that HAB rodents are particularly suited to resolve the apparent discrepancy between the preclinical and clinical findings to date.

Key words: **anxiety; basolateral amygdala; fear; paraventricular nucleus; promoter fragmentation**

Introduction

Anxiety disorders are among the most common psychiatric illnesses, with a lifetime prevalence of ~30% (Kessler and Wang, 2008). While a number of pharmacotherapies are available, the lack of truly novel-acting compounds has led to a focus on the development of non-GABAergic compounds (Cryan and Slattery, 2007). Neuropeptides represent such potential targets due to their distinct synthesis and release sites, and multiple behavioral functions (Landgraf et al., 2007; Slattery and Neumann, 2010a).

Neuropeptide S (NPS) together with its G-protein-coupled receptor, NPS receptor 1 (NPSR1), represent such a candidate system. NPS is synthesized in discrete clusters of brainstem nuclei, including the peri-locus ceruleus area (hereafter termed LC), whereas its receptor exhibits a widespread distribution pattern (Xu et al., 2007; Leonard and Ring, 2011). In rodent studies, central and nasal administration of NPS elicits potent anxiolytic and arousal effects, as well as facilitating the extinction of conditioned fear (Jüngling et al., 2008; Leonard et al., 2008; Meis et al., 2008; Ionescu et al., 2012; Lukas and Neumann, 2012; Wegener et al., 2012).

In humans, *Npsr1* is located in a chromosomal region linked to panic disorder, and a corresponding single nucleotide poly-

Received Nov. 7, 2013; revised Jan. 5, 2015; accepted Jan. 27, 2015.

Author contributions: D.A.S., R.R.N., Y.-C.Y., S.S., G.W., A.A.M., N.S., L.C., R.L., and I.D.N. designed research; D.A.S., R.R.N., T.G., Y.-C.Y., S.B.S., A.F., B.C.F., and B.E. performed research; D.A.S., R.R.N., Y.-C.Y., S.B.S., U.N., R.G., and G.C. contributed unpublished reagents/analytic tools; D.A.S., R.R.N., T.G., Y.-C.Y., S.B.S., A.F., B.C.F., B.E., N.S., L.C., and I.D.N. analyzed data; D.A.S., R.R.N., Y.-C.Y., S.B.S., B.E., G.C., G.W., N.S., L.C., R.L., and I.D.N. wrote the paper.

This work was supported by the Austrian Science Fund FWF P25375 and SFB F4410 to N.S., European Research Council, Bundesministerium für Bildung und Forschung, Elitenetwork of Bavaria (to I.D.N.) and the Deutsche Forschungsgemeinschaft (to I.D.N. and D.A.S.). We thank Professor A. Buschauer (University of Regensburg) for the cell line, and Drs. U. Schmidt and T. Rein for the vectors. We also thank Dr. D. Beiderbeck, R. Maloumby, and M. Nussbaumer for their excellent technical assistance.

*D.A.S. and R.R.N. contributed equally to this work.

The authors declare no competing financial interests.

Corresponding should be addressed to Inga D. Neumann, Department of Behavioral and Molecular Neurobiology, Universitaetsstrasse 31, University of Regensburg, 93040 Regensburg, Germany. E-mail: inga.neumann@biologie.uni-regensburg.de.

DOI:10.1523/JNEUROSCI.4764-13.2015

 0270-6474/15/354599-15$15.00/0

morphism (SNP; Asn^{107}Ile-rs324981) has been associated with increased risk of the overinterpretation of fear (Okamura et al., 2007; Donner et al., 2010; Raczka et al., 2010; Domschke et al., 2011). However, while the preclinical findings to date suggest that increasing NPS levels within the brain reduces anxiety and fear responses, the human Ile^{107} receptor variant exhibits increased surface receptor expression and a 10-fold higher NPS-induced signaling response than the Asn^{107} variant (Reinscheid et al., 2005; Bernier et al., 2006).

To investigate the discrepancy between rodent and human literature, and to test the efficacy of NPS as a potential anxiolytic therapeutic, its behavioral effects have to be confirmed in psychopathological animal models (Landgraf et al., 2007). Wistar rats or CD-1 mice selectively bred for high anxiety-related behavior (HAB; rHABs and mHABs, respectively) versus low anxiety-related behavior (LAB; rLABs and lHABs, respectively) represent such models (Neumann et al., 2010; Sartori et al., 2011a). In addition to their high innate anxiety, HAB mice display enhanced expression, and HAB rats display impaired extinction of conditioned fear responses, respectively (Muigg et al., 2008; Sartori et al., 2011b; Yen et al., 2012). While these behaviors can be attenuated in rHABs with traditional anxiolytics, mHABs do not respond to such treatment (Sah et al., 2012). These inborn differences make these rodents attractive models to further assess the genetic underpinnings of extremes in anxiety-related behavior and the anxiolytic potential of novel drugs (Czibere et al., 2011; Neumann et al., 2011).

Therefore, to address the putative discrepancy between the preclinical and clinical findings regarding the NPS system and anxiety, we tested the hypothesis that selective breeding for anxiety leads to genetic, expressional, and functional differences in the brain NPS–NPSR1 system. We next determined whether NPS administration could exert its anxiolytic and fear extinction effects in these animals with genetically predisposed psychopathologies and limited efficacy of traditional anxiolytics.

Materials and Methods

Animals

Adult male rHAB and rLAB Wistar rats (280–350 g), mHAB and mLAB CD-1 mice (30–35 g) and weight-matched nonselected Wistar rats (rNAB; Charles River) and CD1 mice (mNAB; Munich breeding) were used in these studies. Rats and mice were housed in groups of four, until 1 week before tissue harvesting or undergoing surgical procedures, when they were single housed. Animals were maintained on a 12 h light/dark cycle (lights on: rats, 6:00 A.M.; mice, 8:00 A.M.) in a temperature-controlled colony (21–23°C, 55% humidity). The animals had free access to food and water. All experimental procedures were performed in the morning (8:30–11:30 A.M.). The primary testing for the selection of experimental HAB and LAB rats and mice was performed on the elevated plus-maze (EPM) at the ages of 9 and 7 weeks, respectively, as previously described (Krömer et al., 2005; Neumann et al., 2010). All experiments were conducted with the approval of the local governments of the Oberpfalz and Oberbayern.

Measurement of Npsr1 *and* Nps *mRNA levels, and NPSR1 protein levels*

Rats and mice were killed under basal conditions and brief 20 s isoflurane anesthesia. Brains were snap frozen in *N*-methylbutane stored at −80°C, and LC, paraventricular nucleus (PVN), and amygdala tissue samples were collected. The 3 × 200 μm PVN-targeted, 3 × 200 μm amygdala-targeted, and 5 × 200 μm LC-targeted sections were mounted on slides with the aid of histological staining and atlases (Paxinos and Watson, 1998; Paxinos and Franklin, 2001). Tissue punchers with diameters of 1.8 mm (rats) and 0.8 mm (mice; Fine Science Tools) were used to harvest PVN, amygdala, and LC tissues.

Table 1. List of primers used for mRNA expression studies in the mHABs and mLABs

Gene	Orientation	Primer sequence (5′ → 3′)
Housekeeping genes		
Rpl13a	(+)	CACTCTGGAGGAGAAACGGAAGG
Rpl13a	(−)	GCAGGCATGAGGCAAACAGTC
B2 mg	(+)	CTATATCCTGGCTCACACTG
B2 mg	(−)	CATCATGATGCTTGATCACA
Target genes		
Nps	(+)	TGGTGTTATCCGGTCCTCTC
Nps	(−)	GGACCTTTTCATCGATGTCT
Npsr1	(+)	CTCTTCACTGAGGTGGGCTC
Npsr1	(−)	CCAGTGCTTCAGTGAACGTC

Table 2. List of primers used for mRNA expression studies in the rHABs and rLABs

Gene	Orientation	Primer sequence (5′ → 3′)
Target and housekeeping genes for rat Nps measurements		
Polr2b	(+)	GAAGCCAGGTTAAGAAATCTC
Polr2b	(−)	GACACTCATTCAGCTCACAC
Gapdh	(+)	TGGAGTCTACTGGCGTCTT
Gapdh	(−)	TGTCATATTTCTCGTGGTTCA
Actb	(+)	GGCACCACCATGTACCCAGGC
Actb	(−)	CGATGGAGGGGCCGGACTCA
Nps	(+)	ATCTTAGCTCTGTCGCTGTC
Nps	(−)	CGACGTCTTCTCCAAAATTG
Target and housekeeping genes for rat Npsr1 measurements		
18srRNA	(+)	ACGGACCAGAGCGAAAGCAT
18srRNA	(−)	TGTCAATCCTGTCCGTGTCC
Actb	(+)	TGTCACCAACTGGGACGATA
Actb	(−)	GGGGTGTTGAAGGTCTCAAA
CycA	(+)	AGCACTGGGGAGAAAGGATT
CycA	(−)	AGCCACTCAGTCTTGGCAGT
Gapdh	(+)	TCACCACCATGGAGAAGGC
Gapdh	(−)	GCTAAGCAGTTGGTGGTGCA
Hmbs	(+)	TCCTGGCTTTACCATTGGAG
Hmbs	(−)	TGAATTCCAGGTGAGGGAAC
Hprt1	(+)	GCAGACTTTGCTTTCCTTGG
Hprt1	(−)	CGAGAGGTCCTTTTCACCAG
Rpl13a	(+)	ACAAGAAAAAGCGGATGGTG
Rpl13a	(−)	TTCCGGTAATGGATCTTTGC
Ywhaz	(+)	TTGAGCAGAAGACGGAAGGT
Ywhaz	(−)	GAAGCATTGGGGATCAAGAA
Npsr1	(+)	CTGTTCTCCATCCCCACACT
Npsr1	(−)	GCAGTTGGAAATCACCGTCT

Quantitative PCR

Total rat and mouse RNA was extracted from PVN, amygdala, and LC tissue, and cDNA was prepared and the real-time quantitative PCR (qPCR) for *Nps and Npsr1* performed as previously described (Elfving et al., 2008; Bunck et al., 2009). Briefly, real-time qPCR was performed on cDNA using a QuantiFast SYBR Green Kit (Qiagen) based on the manufacturer's instruction on a LightCycler (Roche Diagnostics) or an Mx3000P (Stratagene). Standard curves were generated, and each experiment was performed in duplicate. Relative transcript concentrations were calculated using the $2(-\Delta\Delta Ct)$ method (Livak and Schmittgen, 2001). For a list of all primers used, see Tables 1 and 2.

Western blotting

Total protein was extracted from PVN-containing tissue punches (separate cohorts from those used for qPCR). Briefly, tissue was homogenized in RIPA buffer (Sigma) supplemented with 0.1 M PMSF, 0.1 M sodium orthovanadate, and protease inhibitor, and incubated on ice for 30 min. After centrifugation (15 min, 14,000 × *g*, 4°C), the supernatant was collected. Protein concentration was measured using the Pierce BCA Protein Assay Kit. Sixty micrograms of rat proteins and 15 μg of mouse

proteins were separated on a 10% SDS-polyacrylamide gel. After transfer onto a nitrocellulose membrane (Bio-Rad), nonspecific binding was blocked in Tris-buffered saline/0.1% Tween-20 (TBST), pH 7.4, supplemented with 5% nonfat milk powder (Sigma) for 1 h at room temperature. The semi-quantitative assessment of NPSR1 protein was performed using an anti-NPSR1 antibody purchased from Abcam (ab92425) or an anti-NPSR1 (Ab2; Leonard et al., 2011), which was provided by Dr. Robert Ring (Pfizer, New York, NY). Membranes containing rat proteins were incubated in Ab2 (1:500) and those containing mouse proteins were incubated in Ab2 (1:500) or ab92425 (1:500) overnight at 4°C with gentle shaking. Thereafter, the membranes were washed three times for 5 min each in TBST, incubated in a 1:1000 dilution of HRP-conjugated anti-rabbit antibody (New England Biolabs) in 2.5% milk in TBST for 30 min at room temperature, washed three times, and visualized by chemiluminescence (Western Lighting, PerkinElmer). β-Tubulin (1:1000) was used as a loading control (New England Biolabs).

Genotyping of NPSR1 knock-out mice

Genomic DNA was prepared from hypothalamic punches of NPSR1 wild-type (WT; NPSR1$^{+/+}$) and NPSR1 knock-out (KO; NPSR1$^{-/-}$) mouse brains (provided by Dr. Chiara Ruzza, University of Ferrara, Ferrara, Italy). DNA was incubated overnight at 55°C and 1000 rpm with horizontal shaking conditions in 200 μl of proteinase K lysis buffer containing 50 mM KCl, 10 mM Tris-HCl, pH 8.3, 1 mM $MgCl_2$, 0.45% Nonidet P-40, 0.45% Tween 20, 0.1 mg/ml gelatin, and 0.5 mg/ml proteinase K. Thereafter, samples were incubated for 10 min at 95°C and centrifuged for 10 min at 14,000 g, 4°C. Two microliters of genomic DNA was added to a PCR mix containing DreamTaq PCR Master Mix (Thermo Scientific) and primers in a final concentration of 0.2 μM. The following three oligonucleotide primers were used: the forward primer was specific to the endogenous NPSR locus [5′-CCTTATCCTCAAACCACGAAGTAT-3′]; the second was a common reverse primer [5′-GTGGGTACATGAGAA GGTTAGGAG-3′]; and the third was a forward primer [5′-AAATG CCTGCTCTTTACTGAAGG-3′] specific to the targeting plasmid. The reaction mix was placed in a thermal cycler and incubated for 5 min at 95°C. The PCR proceeded for 40 cycles as follows: 95°C for 30 s, 55°C for 30 s, and 72°C for 1 min. Additionally, samples were incubated at 72°C for 5 min and was finally stored at 12°C. Amplification products were separated by agarose gel electrophoresis at 140 V for 1 h and then stained with RotiStain (Roth), and images were captured using ChemiDoc XRS system (Bio-Rad).

Nps *and* Npsr1 *sequencing and bioinformatic analysis*

Genomic DNA was extracted from HAB and LAB rodents (NucleoSpin Tissue Kit), and sequencing primers (Tables 3, 4, 5, 6; Sigma-Aldrich) were designed using Primer-BLAST (National Center for Biotechnology Information, Bethesda, MD). Sequencing and bioinformatic analyses were performed as previously described (Bunck et al., 2009). The *Nps* and *Npsr1* DNA fragments (Frags) were amplified using *Taq*-polymerase (Fermentas). Cleaned PCR products were used for sequencing by the Big Dye Terminator kit version 3.1 (Applied Biosystems), and sequences were resolved by capillary electrophoresis on a 3730 DNA analyzer (Applied Biosystems). Rat and mouse *Nps* and *Npsr1* DNA sequences were analyzed using BioEdit version 7.0.2 (Hall, 1999). Transcription factor binding sites in the *Npsr1* promoter were predicted using the Transcription Element Search System (TESS; Schug, 2008). Genomic coordinates are based on genome builds RGSC3.4 (EnsEMBL release 68) for rats and Mm10 (GRCm38, EnsEMBL release 68) for mice.

Copy number variation

The isolated genomic DNA was also used to measure the number of gene copies of *Nps* and *Npsr1* using qPCR. The corresponding primers are listed in Table 7. No cytosine–phosphodiester–guanine (CpG) islands, as assessed using CpG island searcher (Takai and Jones, 2002, 2003), were identified.

Allele-specific transcription assay

PVN and amygdala tissues were punched as described above from F1 offspring of crossed HAB versus LAB rats or mice, respectively. Both crosses (i.e., HAB or LAB father) were performed to rule out imprinting-based effects. Total RNA was isolated, and the converted cDNA was used to quantify HAB and LAB alleles by qPCR, as described above. The primers were designed to differentiate between the HAB and LAB alleles by incorporating the SNPs between the rat (A(227016)G) and mouse (A(156453)G; rs37572071) lines (Table 8) at the 3′ end of the respective primers.

Table 3. List of primers used for sequencing of the rat *Npsr1* gene with location and exons/promoter/downstream enhancing region the primers hybridized to

Sequential order	Location	Orientation	Primer sequence (5′ → 3′)
1	Intron 1	(+)	GGTGAGCAATAGCCAGAAGC
1	Intron 2	(−)	CAGAATTTAAAGCCAGGGCA
2	Intron 2	(+)	GCGCAAGTGACTGTGTCATC
2	Intron 3	(−)	CTTCTCTCCCGCTGGTACTG
3	Intron 3	(+)	TCCATGCCTCACTTTTCCTC
3	Intron 4	(−)	AGCTAGGGAGAAAGGCGTGT
4	Intron 4	(+)	AGCCCAGATCTGCTTCCAGT
4	Intron 5	(−)	ATGGCGTGAGGATCAGGTAG
5	Intron 5	(+)	GTCCTAGTGACTCCCAGCCA
5	Intron 6	(+)	GTTCCCACAAGGAGTTTGGA
6	Intron 6	(−)	TGGCACCTTCAGTATGAGCA
6	Intron 7	(+)	CCAGATACCCCTATTTCCAGC
7	Intron 7	(−)	AGCCGCCACTAATCCATCTT
7	Intron 8	(+)	ACACTCCTTCCCTGCATGTC
8	Intron 8	(+)	AAGAGGGATGCTTCTGGTGA
8	Intron 9	(−)	GAGCATTGGGAGCACAACTT
9	Intron 9	(+)	TGGAGGAAGAGGTCCAGTTG
9	Exon 10	(−)	ATGGTGAAGGTCTGGGTGAG
10	Exon 10	(+)	CTCTCCAAGCCTGAATTCATC
10	Exon 10	(−)	CTAACATCTTCTCCTCCACATG
11	Exon 10	(+)	GGAGGACAACAAAGGTTAGAC
11	Exon 10	(−)	ATAAGACCAGCACTTCCTTG
12	Exon 10	(+)	AAATAGTGATAGACCCTGGC
12	Exon 10	(−)	ACATGTTAACGACTGAACGA
13	Exon 10	(+)	CCCACAGCCCTATGACGCACG
13	Exon 10	(−)	TGCTAGCTAGGACACCCGCCA
14	Exon 10	(+)	GCTGACGGCTCGTTCAGTCG
14	Exon 10	(−)	AGGGGATGGTGTCGGCATGTG
15	Exon 10	(+)	ACAGGACTGGTGCTGAAATCGC
15	Exon 10	(−)	ACTTCAACATCCTCTGCTACACTGC
16	Exon 10	(+)	GTCCTATGATGCTGGATGAATCATGC
16	Exon 10	(−)	CCTGAAAGGAGAGGATCTTTCGCCA
17	Exon 10	(+)	GGTGCCCACCTTCCACACCAAGATG
17	DER	(−)	GGCCATCAGACGTGTGGCTTCC
18	DER	(+)	CCAGCTTCATAGAGACAGCTCTGC
18	DER	(−)	ACCCCCATTCTCCCACCCCAC
19	DER	(+)	TCATTATCCACAACAGGGCTGGACC
19	DER	(−)	ATGGCCTGCAAGGCTAAGGCG
20	DER	(+)	CAGCACTTGGGAGACAGAGA
20	DER	(−)	TGCTGAGCTAAATGTCAAAG
−1	Promoter	(+)	AGACAAACACAGACCCCTGC
−1	Intron 1	(−)	GAGTTCAGTTAGCCAGGGCA
−2	Promoter	(+)	TGTCATGTCGAAACCCTTCA
−2	Promoter	(−)	CAGCTGAGATCGCTTTTGTCT
−3	Promoter	(+)	GTCAGCAGCTTCTGTGCATC
−3	Promoter	(−)	AAGGGGTATGTCCCAGGAAG
−4	Promoter	(+)	TGCACCCATTTTTAGTTCCC
−4	Promoter	(−)	AGGGGTATGTCCCAGGAAGT
−5	Promoter	(+)	GATCCTACTTTGGGCCTGTCG
−5	Promoter	(−)	GAAGATGCTCAACCACATTATTAGC
−6	Promoter	(+)	GTCCACCCCTGAGAGTTCCAG
−6	Promoter	(−)	CAGGGCATCAAGTGAGGGCATC
−7	Promoter	(+)	GGTGTGGATTTGTGAGGGAGGT
−7	Promoter	(−)	GTTCAGTCAGGGAAGATGCATC

DER, Downstream enhancing region.

Dual luciferase assays

Npsr1 *promoter constructs.* Homologous *Npsr1* sequences of HAB and LAB animals were cloned into pGL3 basic luciferase vectors and trans-

Table 4. List of primers used for sequencing of the mouse *Npsr1* gene with location and exons/promoter/downstream enhancing region

Sequential order	Location	Orientation	Primer sequence (5′ → 3′)
−7	Promoter	(+)	GCAGAGGAGACCACACTGGCG
−7	Promoter	(−)	GCCTGACGACAAGGAAGATCCACG
−6	Promoter	(+)	TTGTCATCTCCTGTCTGTGCCCCT
−6	Promoter	(−)	CGCCAGTGTGGTCTCCTCTGC
−5	Promoter	(+)	TGCAGCGTAATGAACACCCCCA
−5	Promoter	(−)	GTAGGCCAACCTTTGCTTTACTGCC
−4	Promoter	(+)	CTGTATGTGCAAATGTGTGTC
−4	Promoter	(−)	GGAGAGCAGAATGTCATGAG
−3	Promoter	(+)	AAGCCCTCATCTCTAACCTG
−3	Promoter	(−)	TCATGGTTTCCCCTCCTCCA
−2	Promoter	(+)	GGGCAAACAAACACTATTGATC
−2	Promoter	(−)	ACATCCCCTAAATACCACTGAGT
−1	Promoter	(+)	CACCTACAAACTTTTCCATC
−1	Promoter	(−)	AATCTCCACATTTCCCTGAG
1	Promoter	(+)	GGGCAGGTCTGTGGGATGGTG
1	Intron 2	(−)	GCCTCCCTAGCAGCAGCTAAGACT
2	Intron 2	(+)	CCTGGGCATTTGCTGGGCGG
2	Intron 3	(−)	TGTGAGGACACTGAAGGTGGCA
3	Intron 3	(+)	AGCAAGCCCTCTCCTGGGACC
3	Intron 4	(−)	AAGGAGTGTCTGATTGTGCAGGAC
4	Intron 4	(+)	CTGCTTCCAGCAGGGAGGGC
4	Intron 5	(−)	TGGGGTGAGGATCAGGCAGCA
5	Intron 5	(+)	AGGTAGGTGGGCCTGCACCC
5	Intron 6	(−)	AAGCAGGGTCCAGCCCGTGG
6	Intron 6	(+)	CAAGCAGAGCTGTCAAGGATGGT
6	Intron 7	(−)	GCTTTCAGGGAGGCCGAGTGG
7	Intron 7	(+)	TGGGCATTTGCATTGGGTTGC
7	Intron 8	(−)	TGGCTCTTGCAGCAGTCAAACAC
8	Intron 8	(+)	TGTTAGCACACCCAAGGCCAC
8	Intron 9	(−)	GGAAGTGTACGGAGGTTCGCAGC
9	Intron 9	(+)	ACTGTCCACTAGGCTGTGATGGC
9	Exon 10	(−)	TGCAGGTGCTGGGCTAACGG
10	Exon 10	(+)	TGCCACCTGCAATTCACGCAC
10	Exon 10	(−)	TGTGCCTGCATGGTGTCCTTGT
11	Exon 10	(+)	AGCAAGAGCAAACTCCCAAGCA
11	Exon 10	(−)	GCATCATAGGGCTGTGGGTGG
12	Exon 10	(+)	GGCACCTCTGGCACCTCTGC
12	Exon 10	(−)	CCACCATGACCTTAAGCAGGCAGC
13	Exon 10	(+)	TGGCTGACTGCTGGTTGAGTCG
13	Exon 10	(−)	CAAGGGCCTGGGCCTCCTGT
14	Exon 10	(+)	AGCAAGCAGAAGCATTGAGTGGC
14	Exon 10	(−)	GTGGTGCCCAGAGACACAGCA
15	Exon 10	(+)	GCCATCTATGCAGAACTTGCTCTAG
15	Exon 10	(−)	AACACATTTGCCCGATCAGCCT
16	Exon 10	(+)	AGGTGCCTACCTTCCACACCAAG
16	DER	(−)	GGCTGTCAAATGTGCAGCTTCCCT

DER, Downstream enhancing region.

Table 5. List of primers used for sequencing of the rat *Nps* gene with location and exons/introns/promoter/downstream enhancing region the primers hybridized to

Sequential order	Location	Orientation	Primer sequence (5′ → 3′)
1	Promoter	(+)	CCCCTGGCCACCCATGTCAC
1	Exon2, Intron 2	(−)	AGCCGTGAAGCCCTTACCTTGGA
2	Promoter	(+)	GCAGGCTCAGACAGCGAGCG
2	Intron 2	(−)	GAAACAGCCATTTCCATGTGCAGG
3	Intron 2	(+)	TCAGGATGGTGGAGTGCCCAA
3	Intron 2	(−)	GCTCATGGCATAGGAGCAAGGACA
4	Intron 2	(+)	AAATGATTGCCTTTCTTCGGGGGT
4	Intron 2	(−)	ACACCACCTTGTGGCCCAGGA
5	Intron 2	(+)	TCCAAGTGGCAACTCCTGCAAGC
5	Intron 2	(−)	AGGCAGCACCATCGCTCACC
6	Intron 2	(+)	TGTCCCTAAAGGTTTGCTCACCGC
6	Intron 2	(−)	ACTGCCCATTTTAAGTCTTGAGCCACC
7	Intron 2	(+)	AGTGGCCTCTGGGAAGAGTGG
7	Intron 2	(−)	GCCCTGGCTGAGTGAATGACTGG
8	Intron 2	(+)	TGCACATCTTCTTTCCTCCAGAGCCA
8	Intron 2	(−)	GCCTCCGATGGGAGCTGCTG
9	Intron 2	(+)	TCCCAACCCCCAAACAGAGCG
9	Intron 2	(−)	ACCGGGCCAAAGGAACCTGC
10	Intron 2	(+)	TGGCTCTGGCGCTTGGCTTC
10	Intron 2	(−)	AGCCCTAGGTTTAGCCCCCAGC
11	Intron 2	(+)	CGGCCTGCCCATGCACACTTA
11	Exon 3	(−)	GCCTGGCTGGGCAGGTACTC
12	Intron 2	(+)	GCTGTGTTTCAGTGATGTTTCTCCCCA
12	DER	(−)	GGCGGAAGTTTGAGACAGGTTTGC
13	Exon 3	(+)	ACGGAGTCGGCTCAGGGGTG
13	DER	(−)	CGCTGGCGATCCCTTGCTGC
14	DER	(+)	ACGACGCGTGGGCGTTTCTAC
14	DER	(−)	TGACCTGGCAGGGACAGCGA
15	DER	(+)	CCTGGGTCTGTTTCTCCCCCTC
15	DER	(−)	CTGGAAGCTGGTGCCAAGGATAC
−6	Promoter	(+)	GGAGCTGCAGGCAAAGCCTCA
−6	Promoter	(−)	ACCCAAACCAAGGTTCCTCACCA
−5	Promoter	(+)	GATACAGCAAACAGGAGGGA
−5	Promoter	(−)	TCTCCAAAGAACAGAGCTCC
−4	Promoter	(+)	CAAGAAGAAGGGAAGTGATGTGGCA
−4	Promoter	(−)	AGGACAAGGAGGTGACCCAGCT
−3	Promoter	(+)	CCCAGGCTTCCAGCTTGGCA
−3	Promoter	(−)	CGGCAGAGGAAAACGTCAGAGGG
−2	Promoter	(+)	CGGATCCTTGTGCTTGCATGGC
−2	Promoter	(−)	GGCCAGGGGCCTCCAAAGGA
−1	Promoter	(+)	CAGCCCTGTCAGCCTGCATCA
−1	Intron 1	(−)	AGGACCTTGGGTGGGATCTCACAC

DER, Downstream enhancing region.

fected into mouse neuro-2a cells using Exgen 500 *in vitro* reagent (Thermo Scientific; Table 9, primer list). The *Npsr1* promoter constructs were cotransfected with a pRK5-Gaussia-KDEL vector, to normalize transfection efficiency, and an SV40-pGL3 vector was used as a positive control (a gift from Dr. Theo Rein and Dr. Ulrike Schmidt, Max Planck Institute of Psychiatry, Munich, Germany). Selected constructs were stimulated with 1 and 10 μM/5 μl dexamethasone (DEX; Ratiopharm) for 24 h before carrying out the dual reporter assay (Schülke et al., 2010).

Npsr1 *cDNA constructs.* Both rat and mouse HAB/LAB *Npsr1* cDNA were amplified with primers (Table 10) carrying additional FLAG tag sequence using Phusion DNA polymerase (New England Biolabs). Finally, the HAB and LAB *Npsr1* cDNAs were cloned into the XhoI/BamHI sites of pcDNA3.1/Zeo$^{(-)}$ (Life Technologies GmbH). Previous studies have shown that NPSR1 signals via the cAMP pathway (Reinscheid et al., 2005); thus, we used a cell line stably expressing a cAMP response element (CRE) cloned upstream of a luciferase reporter (HEK293-CRE-luc; Nordemann et al., 2013) to test the functional properties of HAB and LAB *Npsr1* pcDNA constructs. The HEK293-CRE-luc cells were seeded at 2.5×10^4 cells/well in a 96-well plate with DMEM containing 10% FBS, 1% sodium pyruvate, and hygromycin B (200 μg/ml; Sigma-Aldrich). Twenty-two hours later, cells were replaced in media containing no hygromycin B, and then transfection was performed using 30 ng of HAB/LAB Npsr1 pcDNA constructs and 70 ng Gaussia vector per well using lipofectamine 2000 (Life Technologies). The cells were stimulated with 1 nmol/5 μl NPS (Bachem) 40 h after transfection, and then the dual luciferase assay was performed at 48 h after transfection.

Oligonucleotide pull-down assay

To further determine the functionality of the SNP in the promoter region (rHAB, −388; mHAB, −506), we performed oligonucleotide pull-down assays to assess glucocorticoid receptor (GR) binding.

5′-biotinylated forward oligonucleotides, containing either the HAB or LAB sequence variant with putative GR binding properties, and their respective complementary nonbiotinylated strands (Table 11) were resuspended to a final concentration of 20 μM, and then 5 μl each of forward and reverse primer and 5 μl of 10× NEB buffer 2 were diluted up to 35 μl with distilled water. The reaction mix was incubated for 4 min at 95°C and 10 min at 70°C, and was allowed to cool at room temperature

Table 6. List of primers used for sequencing of the mouse *Nps* gene with location and exons/promoter/downstream enhancing region

Sequential order	Location	Orientation	Primer sequence (5′ → 3′)
−4	Promoter	(+)	CCAGGCTTCCAGCTTGGCAC
−4	Promoter	(−)	GCTGCTATTGCTGCTGTTTCTGAAG
−3	Promoter	(+)	GGGTATCTTTGCCCTCCAAAAGGTG
−3	Promoter	(−)	GGCAATCTGTTGTCACTGGTCCCTG
−2	Promoter	(+)	TCCCTGCTCAACACCCCAAACC
−2	Promoter	(−)	ACTGGTTGGCCTGGCTGTGG
−1	Promoter	(+)	GAGGCTCCTGGCCACCCATG
−1	Intron 2	(−)	GGGCCCTCCACCATCCTGATCA
1	Promoter	(+)	TGGCAAGCTCTGAGTGAAGTCAACC
1	Intron 2	(−)	TTTGGGCCCTCCACCATCCTGA
2	Promoter, Exon 1	(+)	CCCATCTGCGCAGGTCTCGG
2	Intron 2	(−)	TCCACTGTGCGGGTTTTTGGT
3	Promoter, Exon 1	(+)	CATCTGCGCAGGTCTCGG
3	Intron 2	(−)	CCAGAGTTACCTACTGTCACATAC
4	Intron 2	(+)	AGCCGGTGGTAGCCCTACACT
4	Exon 3	(−)	ACTCTGAGCCCGTTAGGAGAAGGG
5	Exon 3	(+)	CCTTTCGCAACGGAGTCGGCT
5	Exon 3	(−)	CGAGCCCTTGCTGCAGGTACC
6	Exon 3	(+)	GTGCCACCAAGTGCAGTGGC
6	DER	(−)	GCTGGTGACCAAGGACAGGGT

DER, Downstream enhancing region.

Table 7. List of primers used for the measurement of copy number variations of *Nps* and *Npsr1* sequence

Species, gene	Orientation	Primer sequence (5′ → 3′)
Rat, *Npsr1*	(+)	GCTGCTGCTGCCCTGGCTAA
Rat, *Npsr1*	(−)	GCCCTCTGTGAGGTTGGCCG
Rat, *Nps*	(+)	AGCTCTGTCGCTGTCCGTGGT
Rat, *Nps*	(−)	AGCCGTGAAGCCCTTACCTTGG
Rat, *Gapdh*	(+)	CGTGTGTAGCGGGCTGCTGT
Rat, *Gapdh*	(−)	CCAGGCGTCCGATACGGCCA
Mouse, *Npsr1*	(+)	CAGCTGCTGCCCCGGCTAAC
Mouse, *Npsr1*	(−)	GGTTGGCTGGCATGGCTCAGG
Mouse, *Nps*	(+)	ACGTGCTTTGGTGTTATCCGGTCC
Mouse, *Nps*	(−)	TTGGGCCCTCCACCATCCTGA
Mouse, *Gapdh*	(+)	TCCCCCTATCAGTTCGGAGC
Mouse, *Gapdh*	(−)	AGTAGCTGGGCCTCTCTCAT

Table 8. List of primers used for allele specific quantification of HAB and LAB alleles in F1 offspring of rats and mice

Species, gene, specificity	Orientation	Primer sequence (5′ → 3′)
Rat, *Npsr1*, common	(+)	ACTGTGGCCAGACGACTCCT
Rat, *Npsr1*, rHAB-specific	(−)	CCTCGGTTGTAGCTGCAGCATATC
Rat, *Npsr1*, rLAB-specific	(−)	CCTCGGTTGTAGCTGCAGCATACT
Mouse, *Npsr1*, common	(+)	GTGCTGTTCTCCACGTGCAG
Mouse, *Npsr1*, mLAB-specific	(−)	TCAGGGGCCATGAAGTCTCGT
Mouse, *Npsr1*, mHAB-specific	(−)	TCAGGGGCCATGAAGTCTCGC

for several hours to allow annealing of the oligonucleotides. Streptavidin beads (GE Healthcare Europe GmbH) were washed with 1 ml of ice-cold PBS and incubated with the annealed 5′-biotinylated oligonucleotides overnight. Nuclear extracts were prepared from total brain tissue from a Wistar rat subjected to restraint stress (by placing it in a Plexiglas restrainer for 30 min and killing it an hour later) using the NE-PER nuclear and cytoplasmic extraction reagent (Piercenet). The extract was precleared using streptavidin beads overnight at 4°C, and the protein concentration was estimated using the Pierce BCA Protein Assay Kit (Thermo Scientific). Then, 300 μg of precleared nuclear proteins was incubated with the biotinylated double-stranded streptavidin Sepharose complex for 4 h at room temperature on a rotating shaker. Afterward, the entire complex was washed twice with RIPA buffer to remove unbound proteins, heated at 95°C in sample buffer, and then separated on 10%

Table 9. List of primers used for cloning rHAB/rLAB and mHAB/mLAB *Npsr1* promoter fragments into luciferase vector

Species, gene, designation	Orientation	Primer sequence (5′ → 3′)
Rat, *Npsr1*, Frag E	(+)	ATCGGTACCGATGGTGAGGGCTGTGCTGG
Rat, *Npsr1*, Frag D	(+)	ATCGGTACCCGATCTCAGCTGAAACAAACTCATAACTC
Rat, *Npsr1*, Frag C	(+)	ATCGGTACCCTCTAGGAATGCACACTTACTCAGCTCTG
Rat, *Npsr1*, Frag B	(+)	ATCGGTACCCCCACTCTAGGGCCTTTCATCTAGG
Rat, *Npsr1*, Frag A	(+)	ATCGGTACCCTGGGTCCTCCAGTCTCTTGAGG
Rat, *Npsr1*, common	(−)	CAGGCTAGCGGCTCAGGCAGGGTCAAGTCTTA
Mouse, *Npsr1*, Frag S	(+)	ATCGGTACCGTGATACCAGCTGAAACAAACACATAACTAC
Mouse, *Npsr1*, Frag R	(+)	ATCGGTACCGAGACAAACACAGACTCCTACCTC
Mouse, *Npsr1*, Frag Q	(+)	ATCGGTACCGCAAAGGTTGGCCTACATGGCTC
Mouse, *Npsr1*, Frag P	(+)	ATCGGTACCGGATTGTCATCTCCTGTCTGTGCC
Mouse, *Npsr1*, common	(−)	CAGGCTAGCGGCTCAGGCAGGGTCAGGTC
–, –, RVprimer3	(+)	CTAGCAAAATAGGCTGTCCC
–, –, GLprimer2	(−)	CTTTATGTTTTTGGCGTCTTCCA

Table 10. List of primers used for cDNA amplification of rat and mouse *Npsr1* cDNA sequences with additional FLAG tag

Species, gene, designation	Orientation	Primer sequence (5′ → 3′)
Rat, *Npsr1*, cDNA	(+)	CATGCTCGAGGCCACCATGCCGGCCAACCTCACA GAGGGCA
Rat, *Npsr1*, cDNA with FLAG	(−)	CATGGGATCCTTACTTGTCGTCATCGTCTTTGTAGT CGATGAATTCAGGCTTGGAGA
Mouse, *Npsr1*, cDNA	(+)	CATGCTCGAGGCCACCATGCCAGCCAACCTCACA GAGGGCA
Mouse, *Npsr1*, cDNA with FLAG	(−)	CATGGGATCCTTACTTGTCGTCATCGTCTTTGTA GTC GATGAATTCCGGCTTGGAGA
–, –, T7	(+)	TAATACGACTCACTATAGGG
–, –, Bgh	(−)	TAGAAGGCACAGTCGAGG

Table 11. List of primers used for oligonucleotide pull-down assay

Species, gene, designation	Orientation	Primer sequence (5′ → 3′)
Mouse, *Npsr1*, mLAB-506 specific	(+)	ACATAACTGACAGATT
Mouse, *Npsr1*, mLAB-506 specific	(−)	AATCTGTCAGTTATGT
Mouse, *Npsr1*, mHAB-506 specific	(+)	ACATAACTCTGACAGATT
Mouse, *Npsr1*, mHAB-506 specific	(−)	AATCTGTCAGAGTTATGT
Rat, *Npsr1*, rHAB-388 specific	(+)	TGGAAACTAGAAGAGAGA
Rat, *Npsr1*, rHAB-388 specific	(−)	TCTCTCTTCTAGTTTCCA
Rat, *Npsr1*, rLAB-388 specific	(+)	TGGAAACTGGAAGAGAGA
Rat, *Npsr1*, rLAB-388 specific	(−)	TCTCTCTTCCAGTTTCCA

SDS-PAGE gels. The separated proteins were blotted on a nitrocellulose membrane, blocked for nonspecific binding using 5% milk-TBST for 1 h, and incubated overnight with a polyclonal GR antibody (sc-1004X, Santa Cruz Biotechnology) at 1:200 dilution in 2.5% milk in TBST. The next day, the blot was washed three times for 5 min with TBST and then incubated for 1 h at room temperature in an anti-rabbit HRP-conjugated secondary antibody (1:1000) dilution in 2.5% milk/TBST. Subsequently, the blot was washed three times for 5 min each in TBST, and proteins were visualized by chemiluminescence (Western Lighting, PerkinElmer). Finally, the blot was also subjected to colloidal silver staining (Harper and Speicher, 2001) to serve as the protein loading control.

Surgical and infusion procedures

Rats and mice were fixed in a stereotaxic apparatus and implanted with an indwelling guide cannula using isoflurane anesthesia under semi-sterile conditions, as previously described (Slattery and Neumann, 2010b; Kessler et al., 2011). A guide cannula (rat: 21 gauge, 12 mm long; mice: 23 gauge, 8 mm long) was implanted 2 or 1.5 mm above the right lateral ventricle [rat: anteroposterior (AP), −1.0 mm from bregma; mediolaterial (ML), +1.6 mm; dorsoventral (DV), +1.8 mm; Paxinos and Watson, 1998; mice: AP, −0.3 mm; ML, +1.1 mm; DV, +1.6 mm;

Franklin and Paxinos, 2007] and anchored to two stainless steel screws using dental acrylic. Animals were allowed to recover for at least 7 d before undergoing behavioral testing and injected with either vehicle (rats, 5 μl; mice, 2 μl of Ringer's solution), NPS (0.1 or 1 nmol) or the NPSR1-antagonist (NPSR1-A) D-Cys(^{t}Bu)^{5}-NPS (10 nmol; Guerrini et al., 2009; rats, 45 min before the anxiety tests or 20 min before fear extinction training; mice, 25 min before behavioral tests). Cannula placements were verified as previously described (Muigg et al., 2008), leading to the exclusion of three HAB mice from further analysis.

Elevated plus-maze

The EPM was used to assess anxiety-related behavior in both rats and mice, as previously described (Krömer et al., 2005; Slattery and Neumann, 2010b). The 5 min test was performed on a plus-shaped maze, which was elevated (rats, 70 cm; mice, 37 cm) from the floor and consisted of two closed arms (rats: 50 × 10 × 40 cm; 25–30 lux; mice: 30 × 5 × 15 cm; 10 lux) and two open arms (rats: 50 × 10 cm; 90–100 lux; mice: 30 × 5 cm; 300 lux) connected by a central neutral zone (rats: 10 × 10 cm; mice: 5 × 5 cm). A camera above the maze enabled the assessment of behavior. The test started by placing the animal in the neutral zone facing a closed arm. During the test, the percentage of time spent on the open arms, as indicative of anxiety-related behavior, and the number of closed arm entries (rats) or total distance traveled (mice; Anymaze software, Stoelting), as indicative of locomotor behavior, were determined by an observer blind to treatment.

Light-dark box

This test was used to assess anxiety-related behavior in nonselected Wistar rats to confirm the anxiolytic effect of NPS. Briefly, the experimental setup consisted of one lit (40 × 50 cm, 350 lux) and one dark (40 × 30 cm, 70 lux) compartment connected via a small opening (7.5 × 7.5 cm), enabling transition between the compartments. The floors in each compartment were divided into squares (10 × 10 cm). Rats were placed in the dark compartment, and the time spent in the light compartment and the number of line crosses were assessed during the 5 min test. The time spent in the light compartment was used to assess anxiety-related behavior, and the number of line crosses as an indicator of locomotor activity (Slattery and Neumann, 2010b).

Auditory fear conditioning

The auditory fear-conditioning experiment was performed according to previous protocols for mice (Sartori et al., 2011b) and rats (Muigg et al., 2008) involving 120 s of stimulus-free habituation, and consolidation periods before and after the last stimulus presentations in all experimental sessions.

Mice acquired conditioned fear by the pairing of five audible cues [conditioned stimulus (CS); white noise, 80 dB, 2 min] and coterminating mild, short, scrambled foot shocks [unconditioned stimulus (US); 0.7 mA, 2 s] in conditioning chambers (TSE). Twenty-four hours later, three CSs in the absence of the US separated by 5 s were presented to mice for a fear expression test in a novel context (single mouse cage, illuminated with red light to 10 lux).

Rats also received five-tone CSs (white noise, 80 dB, 30 s) that each coterminated with a US (0.7 mA scrambled foot shock, 2 s) in the conditioning context (26 × 30 × 32 cm chamber cleaned with water and illuminated to 300 lux; Coulbourn Instruments). Twenty-four hours later, rats were exposed to 30 CSs in the absence of the US, each separated by an intertrial interval of 5 s for extinction training of cued conditioned fear in a novel context (standard rat cage swiped with ethanol and illuminated with red light to 10 lux). On the third day of the experiment, only three CSs were presented to rats in the extinction context.

The time remaining in freezing behavior during acquisition, fear expression test, and fear extinction training was manually assessed by an observer blind to treatment. Freezing scores during fear expression and during extinction, respectively, were binned into three-block averages. The percentage change in freezing behavior between the first-trial block of the extinction training and the extinction retrieval session was used as an indicator of fear reduction induced by the training and/or drug treatment. Animals showing >25% freezing to the context prior to the first CS presentation were excluded from the analysis.

Statistical analyses

Data were analyzed using either ANOVA (one-way, two-way, or two-way with repeated measures) followed by Fisher's least significant difference *post hoc* test or an unpaired *t* test. Statistical significance was set to $p < 0.05$ and performed using SPSS version 19.0.

Results

HAB rodents display lower *Npsr1* mRNA expression and numerous polymorphisms compared with LAB rodents

Initial evidence for a role of the NPSR1 system in the phenotype of the breeding lines was provided by the demonstration of lower expression levels within the PVN and amygdala of HAB rodents compared with their LAB counterparts. rHABs displayed lower *Npsr1* mRNA expression than rLABs only in the PVN ($p < 0.001$; Fig. 1*A*), and mHABs had lower expression only in the basolateral amygdala compared with mLABs ($p < 0.05$; Fig. 1*B*).

Sequencing of the *Npsr1* gene demonstrated numerous insertions, deletions, and SNPs between both breeding lines (Tables 12, 13). In both rats and mice, the LAB sequence was identical to that of the reference strain (BN/SsNHsdMCW and C57BL/6J). TESS analysis revealed a nuclear factor-1 binding site within 500 bp of the DNA region in rLABs, while it was altered to a GR binding site in the corresponding rHAB position. In the homologous region of the mouse gene, adjacent to an activator protein-1 (AP-1) binding site, an insertion in the mHAB sequence also led to the introduction of a GR binding site. Intriguingly, within the coding region, synonymous SNPs [A(227016)G and A(156453)G; rs37572071] in exons 8 and 4 of rHABs and mHABs, respectively, were observed (Tables 12, 13).

cis-Acting polymorphisms drive higher HAB allelic expression

As the differences in expression could be due to *cis–trans* factor interactions, we assessed HAB and LAB allelic expression in cross-mated F1 offspring. Higher HAB allelic expression, regardless of the maternal line, was observed in the F1 generation (rats: $p < 0.001$; Fig. 1*C*; mice: $p < 0.05$; Fig. 1*D*), which is in apparent contrast to the expression levels reported above.

HAB and LAB rodents differ in *Nps* mRNA expression and sequence

We could show higher *Nps* mRNA expression in the LC of rHABs compared with rLABs ($p < 0.05$; Fig. 1*E*), but no polymorphisms were observed between the rat lines. In contrast, while no mRNA expression differences between mHABs and mLABs were observed (Fig. 1*F*), numerous polymorphisms in the *Nps* gene were found (Table 14). In total, 35 SNPs and one insertion were found within the mLAB *Nps* sequence, whereas the mHAB *Nps* sequence was identical to the reference mouse strain (C57BL/6J). The gene-coding locus of mLAB carried four SNPs, leading to amino acid changes at positions leucine(5)isoleucine, valine(10) isoleucine, and arginine(54)glycine; and a synonymous mutation coding for threonine at position 65 in the amino acid sequence—all before the mature 20 aa peptide (Table 14).

HAB and LAB *Npsr1* promoter assays help explain the mRNA expression differences

In both rats and mice, an equal number of gene copies of *Npsr1* and *Nps* were observed in HAB and LAB (*Nps*: rHABs, 1.1 ± 0.13; rLABs, 1.0 ± 0.06; mHABs, 0.83 ± 0.12; mLABs, 1.0 ± 0.26; *Npsr1*: rHABs, 1.1 ± 0.09; rLABs, 1.0 ± 0.05; mHABs, 0.94 ± 0.21; mLABs, 1.0 ± 0.31), and no CpG islands were detected in

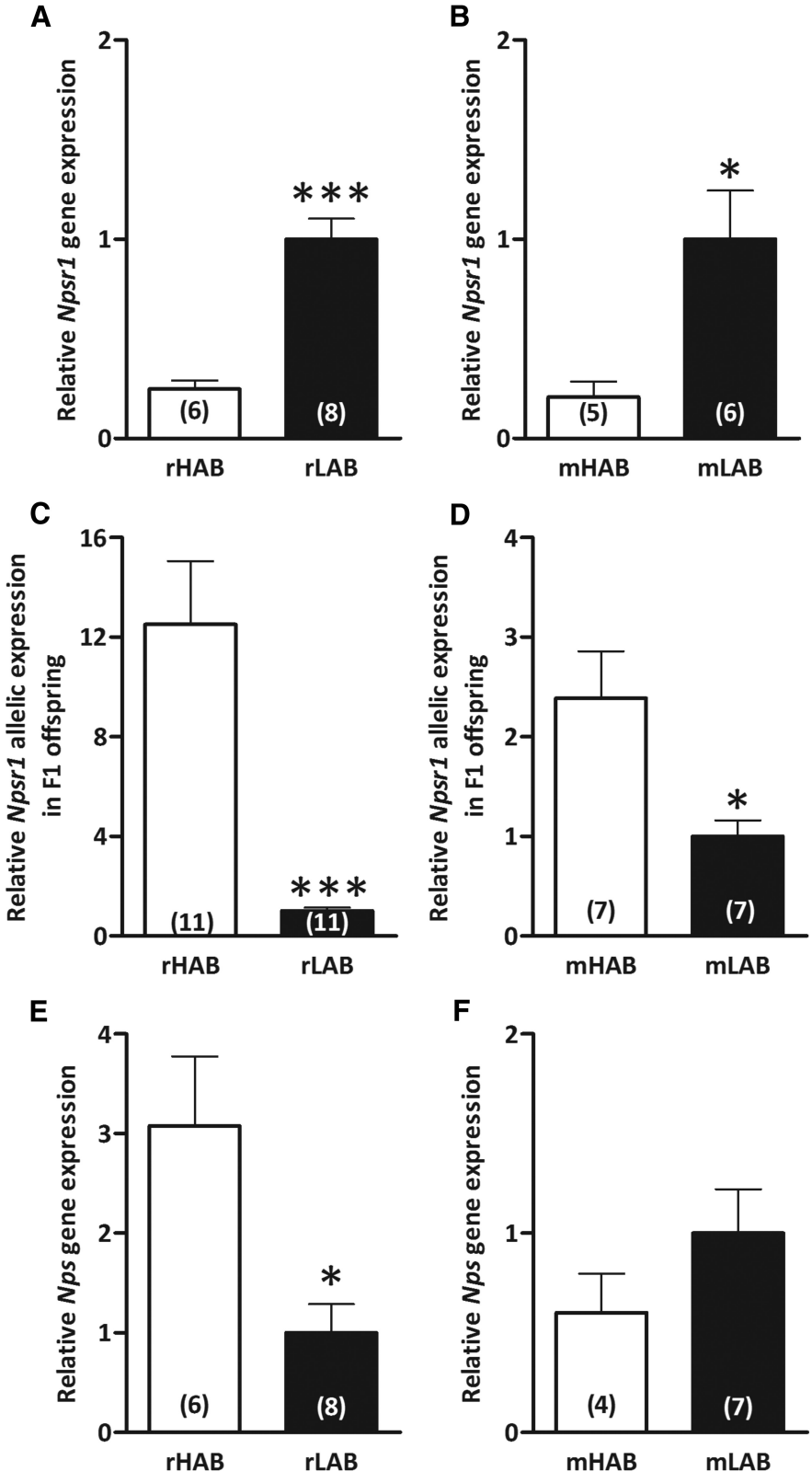

Figure 1. *Npsr1* and *Nps* mRNA expression levels in rats and mice selectively bred for high (rHABs and mHABs) versus low (rLABs and mLABs) anxiety-related behavior, respectively. ***A***, ***B***, Basal *Npsr1* mRNA expression in the hypothalamic PVN in rHABs versus rLABs (***A***), and in the amygdala of mHABs versus mLABs (***B***). ***C***, ***D***, Allele-specific quantification of *Npsr1* alleles using A(227,016)G as a marker to distinguish rHAB- and rLAB-specific alleles in the PVN of F1 offspring (***C***), and using (A(156,453)G; rs37572071) to distinguish mHAB- and mLAB-specific alleles in the amygdala of F1 offspring (***D***). ***E***, ***F***, Basal *Nps* mRNA expression in the locus coeruleus area of rHABs versus rLABs (***E***) and mHABs versus mLABs (***F***). Data are shown as the mean ± SEM, and numbers in parentheses indicate group size. $^{*}p < 0.05$; $^{***}p < 0.001$.

the promoter region of either gene. Thus, to further assess the discrepancy between lower basal HAB *Npsr1* mRNA and higher HAB-specific allelic expression in F1 offspring, we performed dual-luciferase assays. When rat promoter constructs of ~2000 bp upstream of the ATG translation start site were assessed, rHAB activity was approximately half of the corresponding rLAB promoter ($p < 0.001$; Fig. 2*A*). We also assessed the activity of promoter–deletion constructs to deduce the contribution of individual SNPs. No difference was observed between rHAB and rLAB Frag B (−1366 to start codon), while a higher activity in rLABs than rHABs was seen in Frag C (−867 to start codon; $p < 0.01$). These fragments comprise numerous SNPs, making their interpretation difficult, but they do reveal that the SNPs alter promoter activity. However, Frag D (−388 to start codon; containing only one SNP, which introduces a putative GR binding site) had a nearly twofold higher rHAB rat promoter activity in comparison with that in rLABs ($p < 0.001$). Subsequent deletion of the G (−388)A SNP led to Frag E (−221 to start codon) with the C (−221)G SNP, where promoter activity did not differ between rHABs and rLABs (Fig. 2*A*). Similarly, using homologous mouse *Npsr1* promoter constructs, we observed that the activity of the full-length mHAB construct was lower than the corresponding mLAB construct [Frag P (−1193 to start codon); $p < 0.01$]. As the putative promoter length decreased, no difference in the corresponding promoter activity between mHABs and mLABs was observed ≥Frag Q (−845 to start codon) and R (−634 to start codon)]; although, again, interpretation is difficult due to these fragments containing numerous SNPs. However, Frag S (−506 to start codon), which harbors the putative GR binding site and only one SNP, displayed higher mHAB promoter activity than the corresponding mLAB construct ($p < 0.01$; Fig. 2*B*). Moreover, while single CpG bases may influence promoter activity, as shown for human NPSR1 (Reinius et al., 2013), these data suggest that the SNPs in *Npsr1* promoter regions are sufficient to explain the observed differences in mRNA expression.

DEX administration reduces the activity of the HAB *Npsr1* promoter

We next assessed the effect of DEX administration on HAB and LAB *Npsr1* promoter activity to determine whether the

Table 12. *Npsr1* polymorphisms in rHAB versus rLAB: SNPs, deletions, and insertions

Variation type	HAB	LAB	Location in *Npsr1* gene	Relative position
SNP	C	G	Promoter	−1926
SNP	T	C	Promoter	−1856
SNP	C	A	Promoter	−1813
SNP	C	T	Promoter	−1593
Insertion	T		Promoter	−1366
Deletion		C	Promoter	−1300
SNP	A	G	Promoter	−908
SNP	G	A	Promoter	−867
SNP	A	G	Promoter	−388
SNP	G	C	Promoter	−221
Deletion		A	Intron 4	168,623
SNP	T	A	Intron 4	198,121
SNP	C	T	Intron 5	198,323
Deletion		CTT	Intron 5	198,338∼198,340
SNP	G	A	Exon 8	227,016
SNP	C	T	Intron 8	227,154
SNP	C	T	Exon 10	231,601
Deletion		C	Exon 10	231,993
Insertion	AGAGAGAGAGAG		Exon 10	232,152
SNP	C	T	Exon 10	232,218
SNP	C	T	Exon 10	232,505
Insertion	TGTCTCTCTCT		DER	234,193
SNP	A	G	DER	234,331
SNP	A	G	DER	234,985
SNP	C	T	DER	235,041
SNP	G	A	DER	235,223
SNP	T	C	DER	235,279

Positions are relative to the ATG start codon. DER, Downstream enhancing region.

predicted GR binding site close to the ATG start codon in the HAB rodents was functional. In keeping with our *in silico* data, the high activity of HAB Fragments D ($F_{(3,16)} = 3.37$; $p = 0.045$) and S ($F_{(3,16)} = 4.12$; $p = 0.023$), which was recapitulated here ($p < 0.001$ for all HAB vs LAB comparisons), could be reduced by DEX administration ($p < 0.05$ vs water; Fig. 2*C*,*D*).

Oligonucleotide pull-down assay reveals functional significance of the HAB NPSR1 SNP

We could further show that the GR has significantly higher binding to the mHAB (−506) and rHAB (−388) *Npsr1* promoters compared with the corresponding LAB regions (both $p < 0.05$; Fig. 2*E*,*F*). In addition to the expected 95 kDa band size, there were degradation bands at ∼55 and >245 kDa, which represent different antibody-specific immunoprecipitates (i.e., different GR isoforms or binding to their interaction partners).

Synonymous SNP in the HAB rat and mouse NPSR1 coding region causes increased functional activity

Previous studies have shown that synonymous SNPs are not always silent (Duan et al., 2003; Hunt et al., 2009) and that the nonsynonymous SNP in the coding region of NPSR1 leads to increased NPS efficacy and cell surface expression (Bernier et al., 2006). Therefore, we tested the functional impact of the synonymous SNPs in the HAB NPSR1 coding regions by transiently transfecting the HAB versus LAB NPSR1 constructs into cells expressing a luciferase gene downstream of CRE. This assay revealed higher NPS-dependent luciferase expression in cells expressing the HAB NPSR1 protein in both rats and mice compared with transient expression of respective LAB NPSR1 proteins (both $p < 0.05$; Fig. 3*A*,*B*), which is akin to the human Ile^{107} risk isoform. However, we could not determine NPSR1 protein levels owing to the nonspecific nature of the two presently available antibodies, as revealed in genotype-confirmed WT and NPSR1 KO mice (Fig. 3*C*–*E*). Thus, despite an ∼200 bp deletion in the coding region in NPSR1 KO animals, as revealed by Western blot, a 43 kDa band (expected NPSR1 size; ab92425 antibody) or 72 kDa band (Ab2; Leonard and Ring, 2011) were observed in both WT and KO animals. Thus, both the presence of a respective band and the lack of difference in its weight provide evidence for the unspecificity of the currently available NPSR1 antibodies.

Table 13. *Npsr1* polymorphisms in mHAB versus mLAB: SNPs, deletions and insertions

Variation type	HAB	LAB	Location in *Npsr1* gene	Relative position	SNP identifier
SNP	G	A	Promoter	−2251	rs50949943
SNP	C	T	Promoter	−2248	rs48292984
SNP	C	G	Promoter	−2123	rs47083749
SNP	T	C	Promoter	−2112	rs49887483
SNP	T	A	Promoter	−2104	rs47000117
SNP	T	C	Promoter	−2046	rs48022291
SNP	G	A	Promoter	−1942	rs46860992
SNP	T	C	Promoter	−1863	rs51840884
SNP	T	A	Promoter	−1842	rs45839541
SNP	C	T	Promoter	−1775	rs52096988
SNP	G	A	Promoter	−1667	
Deletion		AA (GA) × 18	Promoter	Approximately −1608 to −1571	
SNP	G	A	Promoter	−1516	
SNP	T	C	Promoter	−1469	
SNP	G	A	Promoter	−1418	
SNP	A	G	Promoter	−1376	
SNP	A	T	Promoter	−1315	
SNP	C	T	Promoter	−1236	rs48864073
Deletion		T	Promoter	−1227	
SNP	A	T	Promoter	−1226	rs36643873
SNP	A	T	Promoter	−1132	
SNP	T	G	Promoter	−1072	rs51941766
SNP	G	A	Promoter	−1032	
SNP	C	T	Promoter	−860	rs45719875
SNP	G	A	Promoter	−816	rs37067240
SNP	C	T	Promoter	−731	rs50871983
SNP	C	T	Promoter	−714	rs48580633
SNP	T	G	Promoter	−713	rs47842102
SNP	C	G	Promoter	−674	rs46047101
Deletion		T	Promoter	−648	
SNP	T	A	Promoter	−637	rs45879530
SNP	T	C	Promoter	−612	rs51858460
SNP	T	C	Promoter	−591	rs46930781
SNP	C	A	Promoter	−557	rs50633535
Insertion	C		Promoter	−479	
Insertion	T		Promoter	−478	
SNP	A	T	Intron 1	−82	rs48722200
Insertion	A		Intron 3	156,233	
SNP	G	A	Exon 4	156,453	rs37572071
SNP	C	T	Intron 7	205,648	
Deletion		C	Intron 7	205,718	
SNP	T	C	Intron 8	215,240	
SNP	G	C	Intron 9	215,243	
SNP	G	A	Intron 9	215,244	
SNP	A	G	Intron 9	215,245	
SNP	G	A	Exon 10	216,508	rs49543460
SNP	G	A	Exon 10	217,782	rs49030747
SNP	A	G	DER	218,543	

Positions are relative to the ATG start codon. DER, Downstream enhancing region.

Table 14. *Nps* polymorphisms in mHAB versus mLAB: SNPs, deletions, and insertions

Variation type	HAB	LAB	Location in *Nps* gene	Relative position	SNP identifier
SNP	A	T	Promoter	−1031	
SNP	T	C	Promoter	−1030	
Insertion		GTGT	Promoter	−995	
SNP	T	C	Promoter	−924	rs49048062
SNP	A	G	Promoter	−920	rs42460586
SNP	T	C	Promoter	−871	
SNP	C	T	Promoter	−868	
SNP	T	G	Promoter	−867	
SNP	A	G	Promoter	−819	rs50307957
SNP	C	T	Promoter	−788	rs50890340
SNP	G	A	Promoter	−712	rs49326925
SNP	A	C	Promoter	−621	rs52014995
SNP	T	C	Promoter	−316	
SNP	C	T	Promoter	−163	
SNP	C	T	Promoter	−13	rs33467230
SNP	T	A	Exon 2	125	
SNP	G	A	Exon 2	140	
SNP	G	A	Intron 2	250	
SNP	G	A	Intron 2	273	
SNP	A	T	Intron 2	380	
SNP	A	C	Intron 2	460	
SNP	C	T	Intron 2	502	
SNP	A	G	Exon 3	3624	rs33470378
SNP	A	G	Exon 3	3659	rs33470381
SNP	C	T	Exon 3	3937	rs33471194
SNP	A	G	Exon 3	4022	rs33471197
SNP	T	C	Exon 3	4127	rs33471203
SNP	A	G	Exon 3	4155	rs33471946
SNP	C	A	Exon 3	4195	rs50157889
SNP	C	G	Exon 3	4196	rs33466004
SNP	C	T	Exon 3	4215	rs47207120
SNP	A	G	Exon 3	4217	rs46716508
SNP	G	A	Exon 3	4240	rs49462104
SNP	T	C	Exon 3	4264	rs51623072
SNP	T	A	DER	4321	rs33466010
SNP	G	A	DER	4369	

Positions are relative to the ATG start codon. DER, Downstream enhancing region.

Central NPS administration rescues the anxiety-related behavior and fear deficits in HAB rodents

We next determined whether these genetic and functional differences resulted in behavioral consequences of NPS and NPSR1-A administration in HAB and LAB rodents with genetic predisposition to extremes in anxiety. Initially, we confirmed the anxiolytic effect of intracerebroventricular NPS (1 nmol) administration in rNAB rats, as reflected by an increased amount of time spent in the light compartment of the light-dark box (LDB; $p < 0.05$; Fig. 4*A*), whereas the locomotor activity was not altered by NPS (Fig. 4*F*). The anxiolytic effect of intracerebroventricular NPS administration has also previously been shown in nonselected CD-1 mice (Ionescu et al., 2012).

In rHABs, intracerebroventricular NPS administration dose-dependently altered the percentage of time spent in the open arms of the EPM ($F_{(2,26)} = 17.7$; $p < 0.001$) with 1 nmol ($p < 0.001$), but not 0.1 nmol, leading to an anxiolytic effect (Fig. 4*B*); whereas both doses ($F_{(2,26)} = 12.0$; $p < 0.001$) increased the number of closed arm entries (0.1 nmol, $p < 0.01$; 1 nmol, $p < 0.001$; Fig. 4*G*). Central NPS administration also significantly increased the percentage of time spent in the open arms of the EPM in mHABs ($p < 0.001$; Fig. 4*C*) without altering locomotor activity (Fig. 4*H*).

On the other hand, blockade of the endogenous NPS system by intracerebroventricular administration of NPSR1-A (10 nmol) decreased the percentage of time rLABs and mLABs spent on the open arms of the EPM ($p < 0.05$; Fig. 4*D*,*E*), although it did not affect locomotion (Fig. 4*I*,*J*).

We next tested whether intracerebroventricular NPS could reduce the enhanced fear expression and/or facilitate the impaired fear extinction previously described in mHABs (Sartori et al., 2011b; Yen et al., 2012) and rHABs (Muigg et al., 2008), respectively.

Conditioned freezing responses increased in mHABs (pairing: $F_{(1,15)} = 93.0$; $p < 0.001$), but not mLABs (pairing: $F_{(1,16)} = 1.036$; $p = 0.324$; Fig. 5*A*) across the five CS–US pairings, which is in line with our previous study (Yen et al., 2012). Twenty-four hours later, intracerebroventricular NPS completely abolished fear expression in mHABs ($p < 0.001$; Fig. 5*B*), while the NPSR1-A did not alter freezing levels in mLABs ($p = 0.307$; Fig. 5*B*).

In the rat study, rHABs and rLABs acquired cue-conditioned fear to the same extent (pairing: $F_{(1,35)} = 495$; $p < 0.001$; Fig. 5*C*; and rLAB pairing: $F_{(1,14)} = 202$; $p < 0.001$; Fig. 5*E*). Importantly, neither rHABs nor rLABs showed any freezing to the context on day 2 before the first CS presentation (Fig. 5*D*,*F*). While there was no difference in fear expression between rHABs and rLABs ($F_{(1,32)} = 1.17$; $p = 0.288$), vehicle-administered rHABs exhibited a retarded fear extinction compared with vehicle-administered rLABs (group: $F_{(3,29)} = 5.961$; $p = 0.003$; CS: $F_{(9,261)} = 18.4$; $p < 0.001$; Fig. 5*D*), confirming our previous results (Muigg et al., 2008). However, intracerebroventricular NPS administration significantly accelerated fear extinction in rHABs, but not in rLABs (Fig. 5*D*), which was also evident in the extinction retrieval test, as evidenced by a greater reduction in freezing between the first block of extinction training and the extinction retrieval session (line × treatment: $F_{(1,29)} = 10.4$; $p = 0.003$; data not shown). NPSR1-A administration did not affect the decrease in freezing levels displayed by rLABs during fear extinction training (drug: $F_{(1,13)} = 0.669$; $p = 0.428$; CS: $F_{(9,117)} = 19.5$; $p < 0.001$; drug × CS interaction: $F_{(9,117)} = 0.667$; $p = 0.738$; Fig. 5*E*), and between the first block of extinction training and the extinction retrieval test ($p = 0.320$; data not shown).

Discussion

In this study, we demonstrate that selective breeding of rats and mice for extremes in anxiety-like behavior leads to numerous differences in the *Npsr1* gene sequences between HAB and LAB rodents, which, in turn, cause alterations in transcriptional and functional activity. SNPs were observed in the *Npsr1* promoter region in HAB rodents that causes transcriptional inhibition. However, analogous to the effect of the Ile^{107} SNP in the human NPSR1, a SNP in the exonal region of the rHAB and mHAB receptor sequence resulted in increased NPSR1 signal transduction upon agonist exposure. This increase in NPSR1 activity counteracts the effect of the SNPs in the promoter region and rescue NPSR1 function. Indeed, we could demonstrate that NPS administration elicits anxiolytic and fear-attenuating effects in HAB rodents, supporting this hypothesis. Together, these results suggest that attenuated endogenous NPS system activity mediates, at least in part, the anxiety- and fear-related phenotype of HAB rodents.

Given that the NPS system has been implicated in both anxiety and fear regulation, we speculated that genetic differences may contribute to the behavioral phenotypes of HAB and LAB rats and mice. Indeed, we initially demonstrated that *Npsr1* mRNA

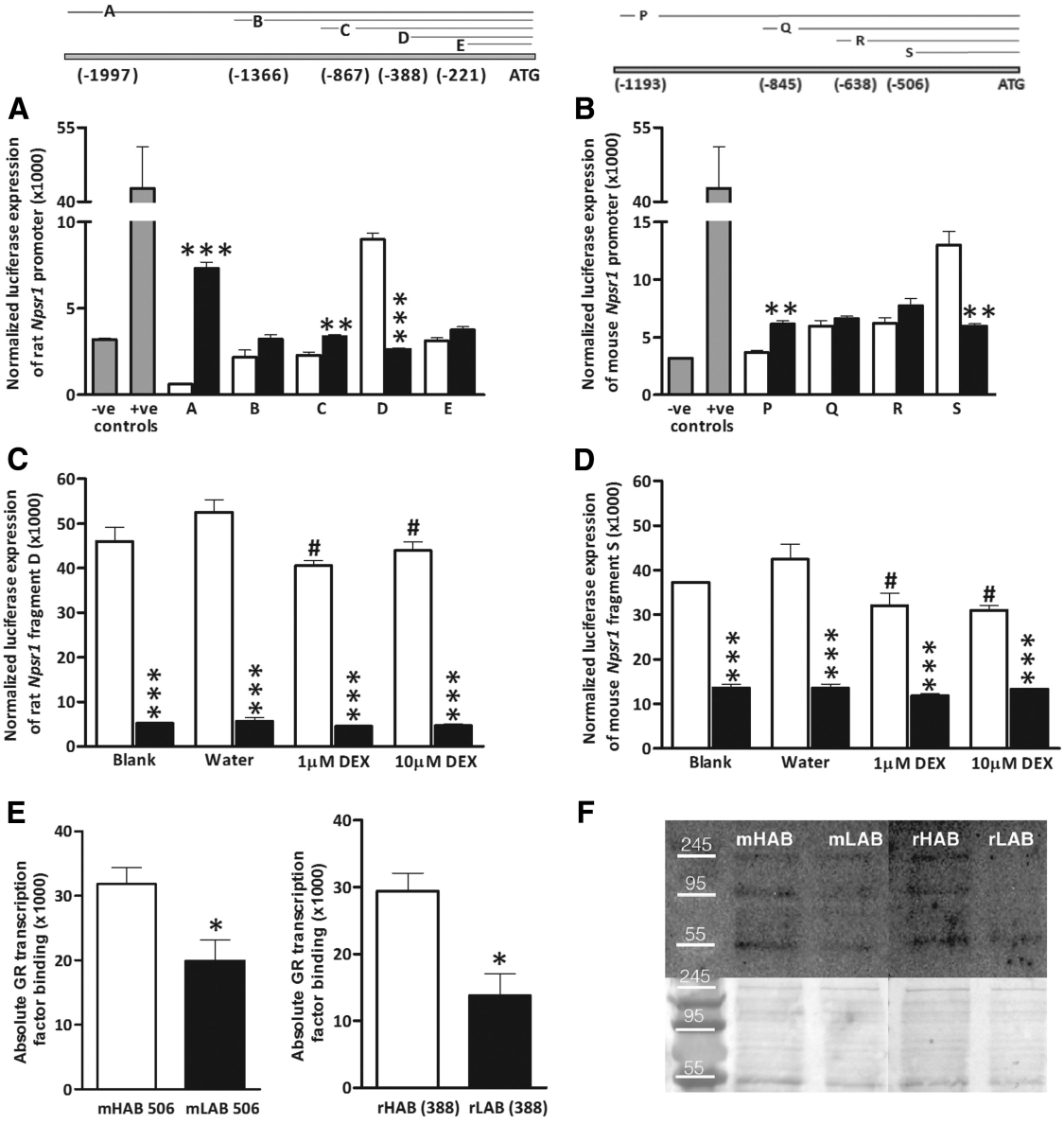

Figure 2. Dual luciferase assays reveal differences in HAB (white columns) and LAB (black columns) rodent *Npsr1* promoter fragments, and pull-down assays show preferential GR binding to the HAB promoter. Fragments displayed in the upper pictogram, with fragments A–E in rats (left), and P–S in mice (right). ***A–D***, Dual luciferase assays of rHAB versus rLAB *Npsr1* promoter constructs in pGL3 basic vector (***A***); mHAB versus mLAB *Npsr1* promoter constructs in pGL3 basic vector (***B***); rHAB versus rLAB fragment D treated with 1, 10 μM DEX, and water as a control for 24 h (***C***); and mHAB versus mLAB fragment S carrying the putative GR binding site treated with 1, 10 μM DEX, and water as control for 24 h before the assay (***D***). ***E***, ***F***, Semi-quantitative Western blots for GR transcription factor binding to mHAB 506 versus mLAB 506 and rHAB 388 versus rLAB 388 (***E***), and representative images with left and right lower images showing corresponding colloidal silver staining (***F***). Data are shown as the mean ± SEM ($n = 3$ for each group and represent independent assays performed in triplicate; except $n = 4$ for Fig. 2*E*); −ve and +ve controls represent pGL3 basic and SV40-pGL3 vectors, respectively. *$p < 0.05$, **$p < 0.01$, ***$p < 0.001$, compared with HAB; #$p < 0.05$, when compared with water.

expression within the PVN (rHABs) and basolateral amygdala (mHABs), regions implicated in local NPS-mediated effects (Smith et al., 2006; Jüngling et al., 2008; Meis et al., 2008), were lower compared with their respective LAB line. Moreover, numerous polymorphisms were also found in the *Npsr1* gene sequence of HABs, while, in contrast, the LAB lines did not differ from their respective reference genomes. While no difference in *Nps* mRNA expression was observed between the mouse lines, we could demonstrate a threefold higher expression level in rHABs compared with rLABs in the LC. In contrast, although no *Nps* sequence differences were observed between the rat lines, polymorphisms in the *Nps* gene leading to 3 aa substitutions within the putative signal peptide sequence of mLABs were identified (Table 11). However, it remains to be determined whether these differences in *Nps* expression and sequence play a role in the rHAB and mLAB phenotypes, respectively.

To discern whether the *Npsr1* polymorphisms underlie the differential mRNA expression between the breeding lines, we next performed dual luciferase assays. These assays recapitulated the *in vivo* findings, as whole HAB rat and mouse constructs had lower promoter activity *in vitro* than their respective LAB constructs, which must be driven by the sequence variation. In contrast, as the putative promoter length was decreased, there was a twofold higher promoter activity in rHABs and mHABs, which is analogous to the higher HAB-specific allelic expression in the F1 offspring. This indicates the importance of the whole promoter, and the cross talk between *cis*-acting polymorphisms and *trans*-acting factors. Intriguingly, TESS analyses revealed the introduc-

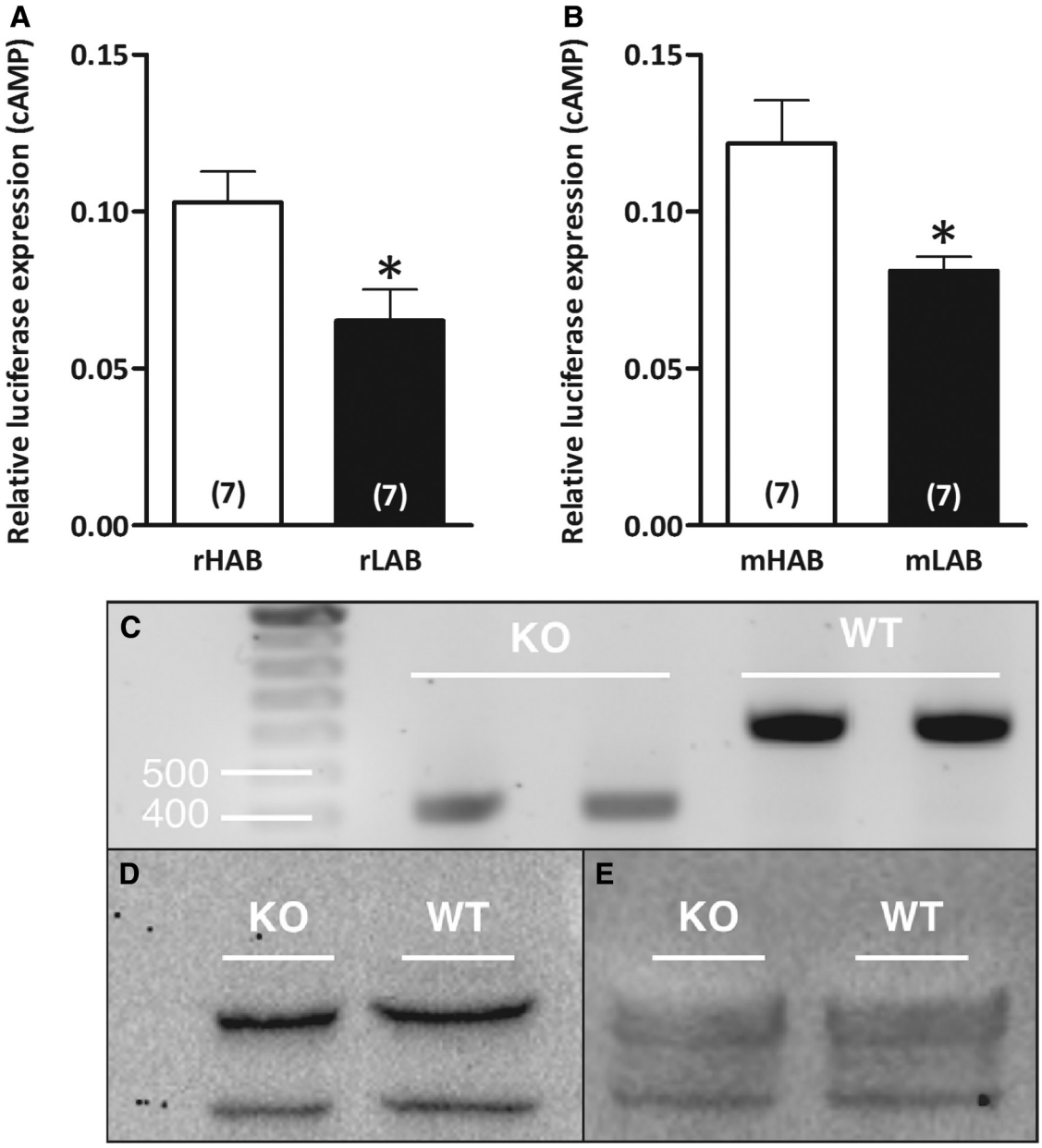

Figure 3. Functional differences in HAB and LAB NPSR1 variants. ***A***, ***B***, HEK-CRE-luc cells were transfected with rHAB or rLAB *Npsr1* cDNA constructs carrying A(227,016)G (***A***) and mHAB or mLAB *Npsr1* cDNA constructs carrying A(156,453)G (***B***); rs37572071 along with Gaussia vector and stimulated with 1 nmol/5 μl NPS at 40 h after transfection until assay at 48 h. ***C***, NPSR1 genotyping using hypothalamic tissue from WT and NPSR1 KO mice. ***D***, ***E***, Semi-quantitative Western blots for total NPSR1 protein of WT and NPSR1 KO mice in hypothalamic paraventricular nucleus tissue with Abcam antibody ab92425 (43 kDa; ***D***) and with Ab2 (72 kDa; Leonard and Ring, 2011; ***E***). β-Tubulin served as a loading control for both Western blots. Data are shown as the mean $\pm$ SEM, and numbers in parentheses indicate the group size. $^{**}p < 0.01$. The luciferase assay was performed independently, and each *n* was an average of three replicates.

tion of a plausible GR binding site in the HAB sequence compared with a nuclear factor (NF)-1 or AP-1 site in the corresponding LAB promoters. A previous study (Mori et al., 1997) showed that GR causes the suppression of downstream interleukin-5 gene expression by interfering with activities of AP-1 or NF-κB. Moreover, the presence of AP-1 and NF-1 has been shown to enhance chromatin accessibility and subsequent GR binding, which in turn helps to recruit other coactivators in the absence of glucocorticoids (Belikov et al., 2004; Biddie et al., 2011). Thus, in HAB rodents it is possible that the adjacent NF-1 or AP-1 site enhances GR binding, and that this would, in turn, recruit other coactivators, leading to enhanced HAB-specific expression of *Npsr1*.

In contrast, DEX stimulation led to GR activation, which interferes with the activity of basal transcription factors like AP-1 and NF-κB, leading to *trans*-repression (Newton and Holden, 2007). Our finding that DEX administration decreased the promoter activity of *Npsr1* in HAB rodents only suggests that such a *cis–trans* interaction is present in this line. Further, using oligonucleotide pull-down assays, we could confirm that the GR binds to this corresponding region of the HAB *Npsr1* promoters. Although synonymous mutations, such as those observed in both rHABs and mHABs, do not lead to an altered amino acid sequence, they have previously been shown to affect mRNA splicing, stability, protein structure, synthesis, and folding (Cartegni and Krainer, 2002; Cartegni et al., 2002). It has been shown that guanine nucleotides are more frequently observed than adenine nucleotides in the third position of synonymous substitutions (Hunt et al., 2009), and that this may impact both the incorpo-

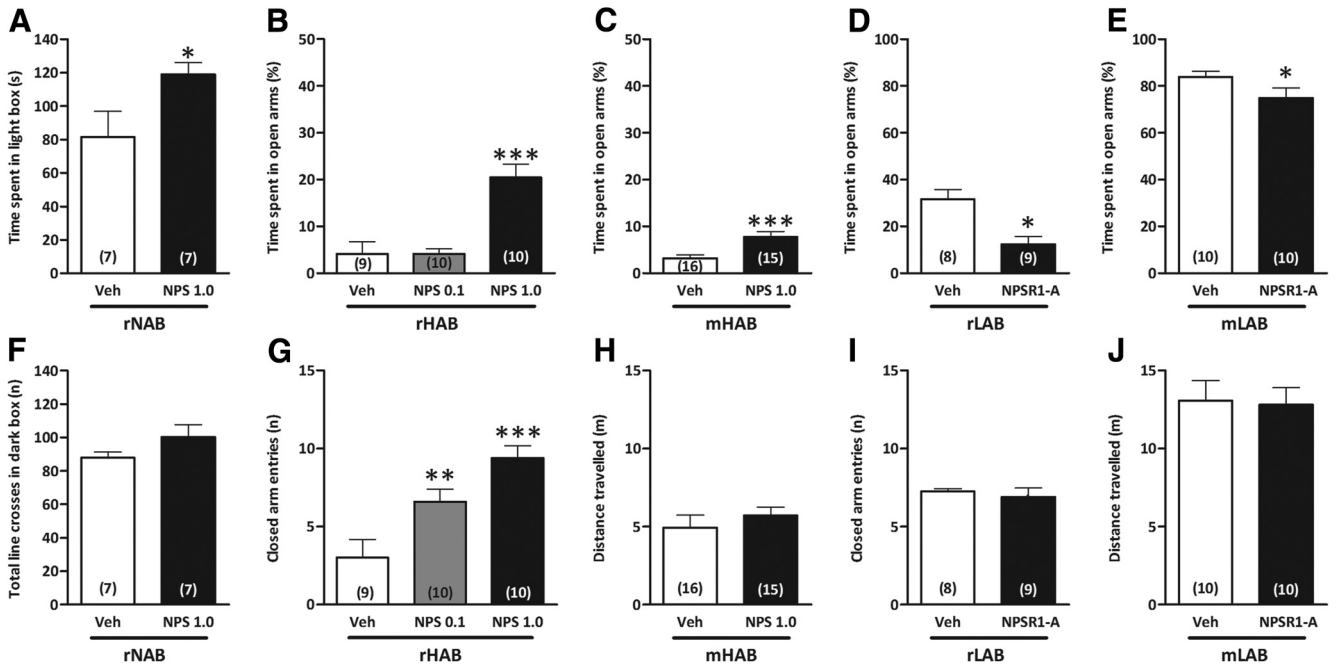

Figure 4. Central NPS and NPSR1-A administration attenuate the anxiety phenotypes of HAB and LAB rodents. ***A–C***, Intracerebroventricular NPS administration exerted an anxiolytic effect in rNABs in the LDB (***A***); in rHABs in a dose-dependent manner, with 1 nmol, but not 0.1 nmol, increasing the time an rHAB spent on the open arms of the EPM (***B***); and in mHABs compared with vehicle treatment (***C***). ***D***, ***E***, Contrastingly, intracerebroventricular administration of D-Cys(tBu)^{5}-NPS (10 nmol), an NPSR1-A, increased the anxiety of rLABs (***D***) and mLABs (***E***) on the EPM. ***F–H***, Intracerebroventricular NPS administration differentially affected locomotor activity with unchanged number of line crosses of rNABs in the LDB (***F***), increased closed arm entries of rHABs on the EPM (***G***), and unchanged distances that mHABs traveled on the EPM (***H***). ***I***,***J***, D-Cys(tBu)^{5}-NPS did not affect locomotor activity in either rLABs (***I***) or mLABs (***J***). Data represent the mean ± SEM. Numbers in parentheses indicate group size. *$p < 0.05$, **$p < 0.01$, ***$p < 0.001$, compared with vehicle group. Veh, Vehicle.

ration rate of amino acids into newly synthesized proteins as well as its subsequent translocation. Such strong codon usage bias has been shown to affect many aspects of gene synthesis in the human dopamine D_2 receptor (Duan et al., 2003). Indeed, we found that both the rHAB and mHAB NPSR1 protein products resulted in greater NPS-induced cAMP response, similar to the human NPSR1 Ile^{107} isoform (Reinscheid et al., 2005). As we could not confirm NPSR1 protein levels, owing to the nonspecific nature of currently available antibodies, two possible explanations for this finding exist. Thus, the synonymous SNP may lead to higher surface receptor expression in HAB rodents, as observed for the human Ile^{107} isoform (Bernier et al., 2006), or it may directly affect NPS–NPSR1 signaling. Future experiments are required to determine which of the two mechanisms is responsible for the HAB NPSR1 phenotype. The findings demonstrating that selective breeding for anxiety leads to alterations in both the *Nps* and *Npsr1* genes and/or expression are intriguing, given the apparent discrepancy between recent preclinical findings of anxiolytic NPS effects and those from human studies. Thus, HAB rodents provide a suitable model to study the effect of NPS administration in animals displaying a similar NPSR1 functional phenotype to that of humans with the Ile^{107} allele. We initially recapitulated and confirmed the anxiolytic effect of intracerebroventricular NPS administration in nonselected Wistar rats (Lukas and Neumann, 2012) and CD-1 mice bred for intermediate anxiety (Ionescu et al., 2012) that has been reported in a number of rat and mouse strains (Xu et al., 2004; Leonard et al., 2008; Rizzi et al., 2008; Wegener et al., 2012). Importantly, we could extend this by demonstrating that even hyperanxiety levels driven by a (seemingly) rigid genetic predisposition and resistance to traditional anxiolytic drugs in mHABs (Sah et al., 2012) are reversed by intracerebroventricular administration of NPS in HAB rats and mice. Although a possible link between anxiety and locomotion has been discussed (Escorihuela et al., 1999), and has been repeatedly described after intracerebroventricular NPS administration (Xu et al., 2007; Ruzza et al., 2012), we could dissociate the anxiolytic and arousal effects of NPS in both HAB rats and mice. Moreover, intracerebroventricular administration of a NPSR1-A (Guerrini et al., 2009) specifically increased anxiety in LAB rats and mice, suggesting an involvement of the endogenous NPS system in the determination of their low innate anxiety levels. This is particularly likely as NPSR1-A administration has not been shown to have an effect on anxiety alone in rodents.

As the Ile^{107} NPSR1 is associated with panic and startle responses in humans (Domschke et al., 2012), we finally determined whether intracerebroventricular NPS administration could reduce conditioned fear expression and facilitate the impaired fear extinction, respectively, in HAB rodents, as shown before in nonselected mice (Jüngling et al., 2008; Meis et al., 2008). Indeed, intracerebroventricular NPS administration was able to reduce the exaggerated fear expression seen in mHABs and to accelerate fear extinction in rHABs. In contrast to the anxiogenic effect observed on the EPM, NPSR1-A administration did not affect fear extinction or fear expression in LAB rats and mice. The fact that NPS administration can rescue the behavioral phenotypes of HAB rodents, coupled with our molecular findings, suggests that a lack of endogenous NPS release may underlie their high anxiety- and fear-like phenotypes. Therefore, we propose that a similar situation may exist in Ile^{107} NPSR1 carriers, given the similar increased NPS-induced signaling in mice, rats, and humans.

In summary, we could reveal genetic differences within the NPS system of rats and mice bred for extremes in anxiety-related behavior, which result in expressional and functional differences.

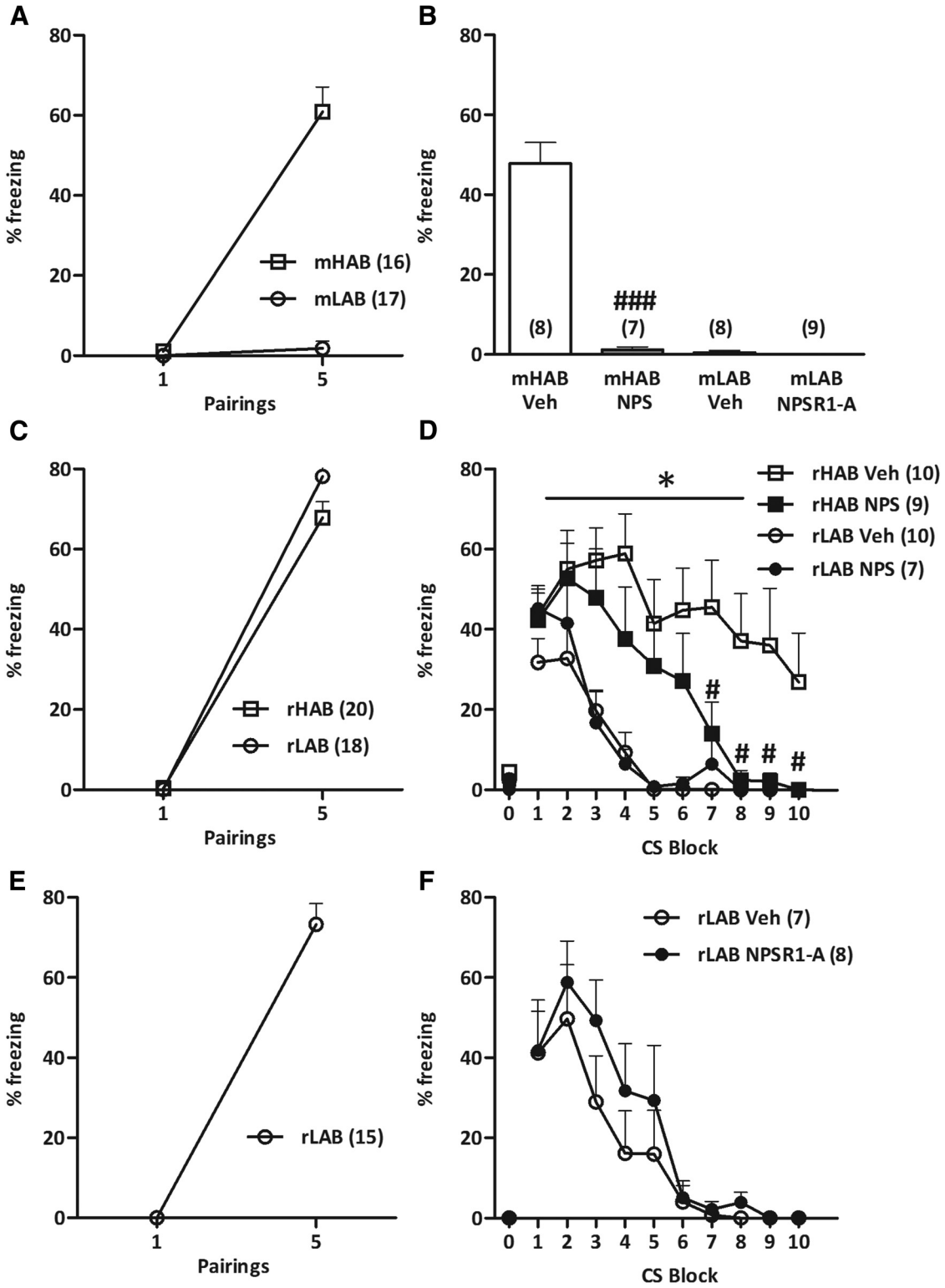

Figure 5. Central NPS administration reverses the cued-fear conditioning deficits of HAB rodents. ***A***, ***C***, ***E***, As a result of acquisition, mHABs (***A***), rHABs, and rLABs (***C***, ***E***), but not mLABs (***A***), showed an increased freezing response to the presentation of the conditioned stimulus (tone). ***B***, ***D***, Twenty-four hours after fear conditioning, intracerebroventricular administration of NPS (1 nmol) 20 min before extinction training completely abolished the expression of cue-conditioned fear in mHABs (***B***) and facilitated the impaired extinction of conditioned fear in rHABs (***D***). ***B***, ***F***, Intracerebroventricular administration of an NPSR1-A (10 nmol) did not alter cued fear expression in mLABs (***B***) or cued fear extinction in rLABs (***F***). ***D***, ***F***, Neither rHABs nor rLABs showed any freezing to the context on day 2 before the first CS presentation. Data represent the mean ± SEM; numbers in parentheses indicate group size. *$p < 0.05$, compared with vehicle-treated LAB animals; #$p < 0.05$ and ###$p < 0.001$, compared with respective vehicle-treated HAB group. Veh, Vehicle.

Moreover, we have shown that synthetic NPS is an efficient anxiolytic agent, even in rats and mice with a strong genetic predisposition to high anxiety, and that it can reverse their deficits in fear extinction. Our findings suggest that differences in the brain NPS system underlie, at least partly, the HAB versus LAB behavioral phenotypes, which seems all the more probable given that functional differences have evolved in both rat and mouse lines, and mirror those in humans with the NPSR1 Ile^{107} allele. Finally, these findings provide evidence to explain the apparent discrepancy between the preclinical and clinical observations to date, and suggest that NPS administration may be particularly effective in anxious patients with the high-risk variant.

References

Belikov S, Astrand C, Holmqvist PH, Wrange O (2004) Chromatin-mediated restriction of nuclear factor 1/CTF binding in a repressed and hormone-activated promoter in vivo. Mol Cell Biol 24:3036–3047. CrossRef Medline

Bernier V, Stocco R, Bogusky MJ, Joyce JG, Parachoniak C, Grenier K, Arget M, Mathieu MC, O'Neill GP, Slipetz D, Crackower MA, Tan CM, Therien AG (2006) Structure-function relationships in the neuropeptide S receptor: molecular consequences of the asthma-associated mutation N107I. J Biol Chem 281:24704–24712. CrossRef Medline

Biddie SC, John S, Sabo PJ, Thurman RE, Johnson TA, Schiltz RL, Miranda TB, Sung MH, Trump S, Lightman SL, Vinson C, Stamatoyannopoulos JA, Hager GL (2011) Transcription factor AP1 potentiates chromatin accessibility and glucocorticoid receptor binding. Mol Cell 43:145–155. CrossRef Medline

Bunck M, Czibere L, Horvath C, Graf C, Frank E, Kessler MS, Murgatroyd C, Müller-Myhsok B, Gonik M, Weber P, Pütz B, Muigg P, Panhuysen M, Singewald N, Bettecken T, Deussing JM, Holsboer F, Spengler D, Landgraf R (2009) A hypomorphic vasopressin allele prevents anxiety-related behavior. PLoS One 4:e5129. CrossRef Medline

Cartegni L, Krainer AR (2002) Disruption of an SF2/ASF-dependent exonic splicing enhancer in SMN2 causes spinal muscular atrophy in the absence of SMN1. Nat Genet 30:377–384. CrossRef Medline

Cartegni L, Chew SL, Krainer AR (2002) Listening to silence and understanding nonsense: exonic mutations that affect splicing. Nat Rev Genet 3:285–298. CrossRef Medline

Cryan JF, Slattery DA (2007) Animal models of mood disorders: recent developments. Curr Opin Psychiatry 20:1–7. CrossRef Medline

Czibere L, Baur LA, Wittmann A, Gemmeke K, Steiner A, Weber P, Pütz B, Ahmad N, Bunck M, Graf C, Widner R, Kühne C, Panhuysen M, Hambsch B, Rieder G, Reinheckel T, Peters C, Holsboer F, Landgraf R, Deussing JM (2011) Profiling trait anxiety: transcriptome analysis reveals cathepsin B (Ctsb) as a novel candidate gene for emotionality in mice. PLoS One 6:e23604. CrossRef Medline

Domschke K, Reif A, Weber H, Richter J, Hohoff C, Ohrmann P, Pedersen A, Bauer J, Suslow T, Kugel H, Heindel W, Baumann C, Klauke B, Jacob C, Maier W, Fritze J, Bandelow B, Krakowitzky P, Rothermundt M, Erhardt A, et al. (2011) Neuropeptide S receptor gene—converging evidence for a role in panic disorder. Mol Psychiatry 16:938–948. CrossRef Medline

Domschke K, Klauke B, Winter B, Gajewska A, Herrmann MJ, Warrings B, Muhlberger A, Wosnitza K, Dlugos A, Naunin S, Nienhaus K, Fobker M, Jacob C, Arolt V, Pauli P, Reif A, Zwanzger P, Deckert J (2012) Modification of caffeine effects on the affect-modulated startle by neuropeptide S receptor gene variation. Psychopharmacology (Berl) 222:533–541. CrossRef Medline

Donner J, Haapakoski R, Ezer S, Melén E, Pirkola S, Gratacòs M, Zucchelli M, Anedda F, Johansson LE, Söderhäll C, Orsmark-Pietras C, Suvisaari J, Martín-Santos R, Torrens M, Silander K, Terwilliger JD, Wickman M, Pershagen G, Lönnqvist J, Peltonen L, et al. (2010) Assessment of the neuropeptide S system in anxiety disorders. Biol Psychiatry 68:474–483. CrossRef Medline

Duan J, Wainwright MS, Comeron JM, Saitou N, Sanders AR, Gelernter J, Gejman PV (2003) Synonymous mutations in the human dopamine receptor D2 (DRD2) affect mRNA stability and synthesis of the receptor. Hum Mol Genet 12:205–216. CrossRef Medline

Elfving B, Bonefeld BE, Rosenberg R, Wegener G (2008) Differential expression of synaptic vesicle proteins after repeated electroconvulsive seizures in rat frontal cortex and hippocampus. Synapse 62:662–670. CrossRef Medline

Escorihuela RM, Fernández-Teruel A, Gil L, Aguilar R, Tobeña A, Driscoll P (1999) Inbred Roman high- and low-avoidance rats: differences in anxiety, novelty-seeking, and shuttlebox behaviors. Physiol Behav 67:19–26. CrossRef Medline

Franklin KBJ, Paxinos G (2007) The mouse brain in stereotaxic coordinates, Ed 3. San Diego: Academic.

Guerrini R, Camarda V, Trapella C, Caló G, Rizzi A, Ruzza C, Fiorini S, Marzola E, Reinscheid RK, Regoli D, Salvadori S (2009) Further studies at neuropeptide s position 5: discovery of novel neuropeptide S receptor antagonists. J Med Chem 52:4068–4071. CrossRef Medline

Hall TA (1999) BioEdit: a user-friendly biological sequence alignment editor and analysis program for Windows 95/98/NT. Nucl Acids Symp Ser 41:95–98.

Harper S, Speicher DW (2001) Detection of proteins on blot membranes. Curr Protoc Protein Sci chapter10:unit 10.8. CrossRef Medline

Hunt R, Sauna ZE, Ambudkar SV, Gottesman MM, Kimchi-Sarfaty C (2009) Silent (synonymous) SNPs: should we care about them? Methods Mol Biol 578:23–39. CrossRef Medline

Ionescu IA, Dine J, Yen YC, Buell DR, Herrmann L, Holsboer F, Eder M, Landgraf R, Schmidt U (2012) Intranasally administered neuropeptide S (NPS) exerts anxiolytic effects following internalization into NPS receptor-expressing neurons. Neuropsychopharmacology 37:1323–1337. CrossRef Medline

Jüngling K, Seidenbecher T, Sosulina L, Lesting J, Sangha S, Clark SD, Okamura N, Duangdao DM, Xu YL, Reinscheid RK, Pape HC (2008) Neuropeptide S-mediated control of fear expression and extinction: role of intercalated GABAergic neurons in the amygdala. Neuron 59:298–310. CrossRef Medline

Kessler MS, Bosch OJ, Bunck M, Landgraf R, Neumann ID (2011) Maternal care differs in mice bred for high vs. low trait anxiety: impact of brain vasopressin and cross-fostering. Soc Neurosci 6:156–168. CrossRef Medline

Kessler RC, Wang PS (2008) The descriptive epidemiology of commonly occurring mental disorders in the United States. Annu Rev Public Health 29:115–129. CrossRef Medline

Krömer SA, Kessler MS, Milfay D, Birg IN, Bunck M, Czibere L, Panhuysen M, Pütz B, Deussing JM, Holsboer F, Landgraf R, Turck CW (2005) Identification of glyoxalase-I as a protein marker in a mouse model of extremes in trait anxiety. J Neurosci 25:4375–4384. CrossRef Medline

Landgraf R, Kessler MS, Bunck M, Murgatroyd C, Spengler D, Zimbelmann M, Nussbaumer M, Czibere L, Turck CW, Singewald N, Rujescu D, Frank E (2007) Candidate genes of anxiety-related behavior in HAB/LAB rats and mice: focus on vasopressin and glyoxalase-I. Neurosci Biobehav Rev 31:89–102. CrossRef Medline

Leonard SK, Ring RH (2011) Immunohistochemical localization of the neuropeptide S receptor in the rat central nervous system. Neuroscience 172:153–163. CrossRef Medline

Leonard SK, Dwyer JM, Sukoff Rizzo SJ, Platt B, Logue SF, Neal SJ, Malberg JE, Beyer CE, Schechter LE, Rosenzweig-Lipson S, Ring RH (2008) Pharmacology of neuropeptide S in mice: therapeutic relevance to anxiety disorders. Psychopharmacology 197:601–611. CrossRef Medline

Livak KJ, Schmittgen TD (2001) Analysis of relative gene expression data using real-time quantitative PCR and the 2(-Delta Delta C(T)) method. Methods 25:402–408. CrossRef Medline

Lukas M, Neumann ID (2012) Nasal application of neuropeptide S reduces anxiety and prolongs memory in rats: social versus non-social effects. Neuropharmacology 62:398–405. CrossRef Medline

Meis S, Bergado-Acosta JR, Yanagawa Y, Obata K, Stork O, Munsch T (2008) Identification of a neuropeptide S responsive circuitry shaping amygdala activity via the endopiriform nucleus. PLoS One 3:e2695. CrossRef Medline

Mori A, Kaminuma O, Suko M, Inoue S, Ohmura T, Hoshino A, Asakura Y, Miyazawa K, Yokota T, Okumura Y, Ito K, Okudaira H (1997) Two distinct pathways of interleukin-5 synthesis in allergen-specific human T-cell clones are suppressed by glucocorticoids. Blood 89:2891–2900. Medline

Muigg P, Hetzenauer A, Hauer G, Hauschild M, Gaburro S, Frank E, Landgraf R, Singewald N (2008) Impaired extinction of learned fear in rats selectively bred for high anxiety—evidence of altered neuronal processing in

prefrontal-amygdala pathways. Eur J Neurosci 28:2299–2309. CrossRef Medline

Neumann ID, Veenema AH, Beiderbeck DI (2010) Aggression and anxiety: social context and neurobiological links. Front Behav Neurosci 4:12. CrossRef Medline

Neumann ID, Wegener G, Homberg JR, Cohen H, Slattery DA, Zohar J, Olivier JD, Mathé AA (2011) Animal models of depression and anxiety: what do they tell us about human condition? Prog Neuropsychopharmacol Biol Psychiatry 35:1357–1375. CrossRef Medline

Newton R, Holden NS (2007) Separating transrepression and transactivation: a distressing divorce for the glucocorticoid receptor? Mol Pharmacol 72:799–809. CrossRef Medline

Nordemann U, Wifling D, Schnell D, Bernhardt G, Stark H, Seifert R, Buschauer A (2013) Luciferase reporter gene assay on human, murine and rat histamine H4 receptor orthologs: correlations and discrepancies between distal and proximal readouts. PLoS One 8:e73961. CrossRef Medline

Okamura N, Hashimoto K, Iyo M, Shimizu E, Dempfle A, Friedel S, Reinscheid RK (2007) Gender-specific association of a functional coding polymorphism in the Neuropeptide S receptor gene with panic disorder but not with schizophrenia or attention-deficit/hyperactivity disorder. Prog Neuropsychopharmacol Biol Psychiatry 31:1444–1448. CrossRef Medline

Paxinos G, Franklin KBJ (2001) The mouse brain in stereotoxic coordinates, Ed 2. San Diego: Academic.

Paxinos G, Watson C (1998) The rat brain in stereotactic coordinates. San Diego: Academic.

Raczka KA, Gartmann N, Mechias ML, Reif A, Buchel C, Deckert J, Kalisch R (2010) A neuropeptide S receptor variant associated with overinterpretation of fear reactions: a potential neurogenetic basis for catastrophizing. Mol Psychiatry 15: 1045, 1067–1074. CrossRef Medline

Reinius LE, Gref A, Sääf A, Acevedo N, Joerink M, Kupczyk M, D'Amato M, Bergström A, Melén E, Scheynius A, Dahlén SE, Pershagen G, Söderhäll C, Kere J (2013) DNA methylation in the Neuropeptide S Receptor 1 (NPSR1) promoter in relation to asthma and environmental factors. PLoS One 8:e53877. CrossRef Medline

Reinscheid RK, Xu YL, Okamura N, Zeng J, Chung S, Pai R, Wang Z, Civelli O (2005) Pharmacological characterization of human and murine neuropeptide s receptor variants. J Pharmacol Exp Ther 315:1338–1345. CrossRef Medline

Rizzi A, Vergura R, Marzola G, Ruzza C, Guerrini R, Salvadori S, Regoli D, Calo G (2008) Neuropeptide S is a stimulatory anxiolytic agent: a behavioural study in mice. Br J Pharmacol 154:471–479. CrossRef Medline

Ruzza C, Pulga A, Rizzi A, Marzola G, Guerrini R, Calo' G (2012) Behavioural phenotypic characterization of CD-1 mice lacking the neuropeptide S receptor. Neuropharmacology 62:1999–2009. CrossRef Medline

Sah A, Schmuckermair C, Sartori SB, Gaburro S, Kandasamy M, Irschick R, Klimaschewski L, Landgraf R, Aigner L, Singewald N (2012) Anxiety- rather than depression-like behavior is associated with adult neurogenesis in a female mouse model of higher trait anxiety- and comorbid depression-like behavior. Transl Psychiatry 2:e171. CrossRef Medline

Sartori SB, Landgraf R, Singewald N (2011a) The clinical implications of mouse models of enhanced anxiety. Future Neurol 6:531–571. CrossRef Medline

Sartori SB, Hauschild M, Bunck M, Gaburro S, Landgraf R, Singewald N (2011b) Enhanced fear expression in a psychopathological mouse model of trait anxiety: pharmacological interventions. PLoS One 6:e16849. CrossRef Medline

Schug J (2008) Using TESS to predict transcription factor binding sites in DNA sequence. Curr Protoc Bioinformatics chapter 2:unit 2.6. CrossRef Medline

Schülke JP, Wochnik GM, Lang-Rollin I, Gassen NC, Knapp RT, Berning B, Yassouridis A, Rein T (2010) Differential impact of tetratricopeptide repeat proteins on the steroid hormone receptors. PloS One 5:e11717. CrossRef Medline

Slattery DA, Neumann ID (2010a) Oxytocin and major depressive disorder: experimental and clinical evidence for links to aetiology and possible treatment. Pharmaceuticals 3:702–724. CrossRef

Slattery DA, Neumann ID (2010b) Chronic ICV oxytocin attenuates the pathological high anxiety state of selectively bred Wistar rats. Neuropharmacology 58:56–61. CrossRef Medline

Smith KL, Patterson M, Dhillo WS, Patel SR, Semjonous NM, Gardiner JV, Ghatei MA, Bloom SR (2006) Neuropeptide S stimulates the hypothalamo-pituitary-adrenal axis and inhibits food intake. Endocrinology 147:3510–3518. CrossRef Medline

Takai D, Jones PA (2002) Comprehensive analysis of CpG islands in human chromosomes 21 and 22. Proc Natl Acad Sci U S A 99:3740–3745. CrossRef Medline

Takai D, Jones PA (2003) The CpG island searcher: a new WWW resource. In Silico Biol 3:235–240. Medline

Wegener G, Finger BC, Elfving B, Keller K, Liebenberg N, Fischer CW, Singewald N, Slattery DA, Neumann ID, Mathé AA (2012) Neuropeptide S alters anxiety, but not depression-like behaviour in Flinders Sensitive Line rats: a genetic animal model of depression. Int J Neuropsychopharmacol 15:375–387. CrossRef Medline

Xu YL, Reinscheid RK, Huitron-Resendiz S, Clark SD, Wang Z, Lin SH, Brucher FA, Zeng J, Ly NK, Henriksen SJ, de Lecea L, Civelli O (2004) Neuropeptide S: a neuropeptide promoting arousal and anxiolytic-like effects. Neuron 43:487–497. CrossRef Medline

Xu YL, Gall CM, Jackson VR, Civelli O, Reinscheid RK (2007) Distribution of neuropeptide S receptor mRNA and neurochemical characteristics of neuropeptide S-expressing neurons in the rat brain. J Comp Neurol 500: 84–102. CrossRef Medline

Yen YC, Mauch CP, Dahlhoff M, Micale V, Bunck M, Sartori SB, Singewald N, Landgraf R, Wotjak CT (2012) Increased levels of conditioned fear and avoidance behavior coincide with changes in phosphorylation of the protein kinase B (AKT) within the amygdala in a mouse model of extremes in trait anxiety. Neurobiol Learn Mem 98:56–65. CrossRef Medline